Contr. Mineral. and Petrol. 37, 307—340 (1972)

Thermal Stability of Al-Fe Epidote as a Function of f_{O_2} and Fe Content

M. J. Holdaway

Department of Geological Sciences, Southern Methodist University, Dallas, Texas 75222

Received July 28, 1972

Abstract. Laboratory experiments have been conducted with natural minerals to determine the relation of f_{O_2} to epidote stability, and to determine stability curves for clinozoisite and epidote. Under oxidizing conditions Fe-epidote decomposes to grandite, anorthite, hematite, and quartz. Under more reducing conditions corundum becomes a stable product instead of quartz, and magnetite, and finally hercynite replace hematite. As conditions change from oxidizing to reducing the temperature of epidote breakdown decreases, epidote becomes more aluminous and the grandite produced increases in grossularite component and, to a lesser extent, in almandine.

At 3000 bars under oxidizing conditions epidote is stable up to 694° C, epidote-corundum is stable to 692° C, clinozoisite is stable to 658° C, and clinozoisite-quartz is stable to 628° C. Approximate curves for the fractional decomposition of Al-Fe epidote have been determined as a function of Fe content under oxidizing conditions. Extrapolation of clinozoisite results to an Fe-free composition, and comparison with zoisite stability results suggest that at elevated pressures clinozoisite inverts with increasing temperature to zoisite along a nearly vertical phase boundary at 635 ± 75° C.

The stability relations provide an upper limit for epidote mineral stability mainly applicable to calcareous rocks. The epidote composition present in any given rock must be a function largely of bulk composition and f_{O_2}. Zoisite replaces Al-clinozoisite in rocks of medium grade and high pressure.

Introduction

Although stability relations of the calcium aluminum silicate minerals are well understood, the effects of ferric iron on the stabilities of solid solution minerals such as epidote and grossularite-andradite are incompletely known. This paper concerns the pressure-temperature-composition-f_{O_2} phase relations of the epidote-group minerals.

Stability relations of the calcium aluminum silicates grossularite and zoisite have been determined by Boettcher (1970), Newton (1965, 1966), and Hays (1967). There is good agreement between these authors; they have demonstrated reversible equilibrium and shown that exploratory results of Pistorius and Kennedy (1960), Pistorius, Kennedy, and Sourirajan (1962), and Winkler and Nitsch (1962) are inaccurate. These recent studies on the calcium aluminum silicate system provide a basis from which to undertake the stability relations of ferric epidote and garnet.

The iron-bearing system has been studied less extensively and to date there has been little agreement between authors. Fyfe (1960a) showed that at 2 kb clinozoisite and epidote could be grown from seeded thermal breakdown products at 605 and 630° C, respectively, whereas clinozoisite seeds disappeared at 715° C. Merrin (1962) made extensive experiments with clinozoisite and epidote compositions using mainly gels in unbuffered gold capsules. He determined PT curves

and observed no effect of Fe content on stability relations, but concluded that such a shift is theoretically probable. Winkler and Nitsch (1963) experimented with synthesized grossularite-andradite, anorthite, and hematite with the composition of clinozoisite-quartz or epidote-quartz. This material was seeded with epidote and placed in unbuffered gold capsules. They showed that Merrin's results were synthesis boundaries (see Fyfe, 1960b), but again detected no relation between Fe content and stability.

Strens (1965) discussed previous work on Al-Fe epidotss and concluded that iron content should raise the breakdown temperature of epidote under oxidizing conditions, such as those of the MH oxygen buffer[1]. He suggested that Winkler and Nitsch (1963) did not notice any difference between clinozoisite and epidote stability because they obtained a partial yield of epidote in all their runs, regardless of composition. In the writer's view, this happened because hematite was always present in the starting materials. Strens suggested that the effect of iron content on stability was about 3° C per mol % pistacite.

Holdaway (1966) studied the clinozoisite-quartz breakdown using the crystal weight method and a MH buffer. The results of that study agreed roughly with those of Winkler and Nitsch (1963) except for disagreement in curve slope. Holdaway (1966) also confirmed Strens' contention that Fe increases the breakdown temperature of epidote minerals.

Starting Materials

Most of the starting materials for this study consisted of natural minerals separated from coexisting phases with the use of heavy liquids and the isodynamic separator. With the exception of the Klamath Mountains garnet (Table 1), none of the minerals shows evidence of variable composition. The Klamath material is zoned over about 9 mol% andradite as indicated by refractive index measurements. Purity of the mineral separates is estimated at 99% or better in each case. Through grinding, sieving, and elutriation minerals were prepared in a grain size range of 10 to 45 μ or 3 to 30 μ. The most recent experiments in the finer range showed a considerable increase in reaction rate without apparently introducing any grain size bias in the results.

Analytical, optical and X-ray data for the epidotes and garnets are presented in Tables 1 and 2. Analyses are an average of two separate atomic absorption analyses for which synthetic standards were made to match the mineral compositions as closely as possible. Analyses are accurate to ±1 to 2% of the amount present. Because the atomic absorption method only gives a value for total iron, the iron was assigned in a somewhat arbitrary manner. In epidote and garnet the following rules were followed: (1) determine metal ion contents on the basis of the number of metal ions in the ideal structural formula; (2) assign Al to fill the remainder of the three Si sites; (3) assign the remainder of the Al and Ti to the octahedral sites; (4) assign Fe to fill the remainder of the octahedral sites; (5) assign remainder of Fe to the 8-fold sites. This procedure assumes that all sites are filled and that Fe is the only ion to be split between octahedral and 8-fold sites. In all cases the contents of Fe, presumably ferrous, in the 8-fold sites is low or nil. The epidotes are very close to an ideal clinozoisite-epidote series, while the garnets all fall near the grossularite-andradite join with less than 3 mol% of any other molecule. In this report epidote will be referred to by the percentage of the hypothetical pistacite molecule (Ps), and the garnet will be referred to by the percentage of andradite (And). Each percentage is determined by dividing octahedral Fe by the sum of octahedral Al and Fe.

Determination of epidote composition in experimental run products was in many cases accomplished through measurement of refractive index, because such measurements could be made on new growth and the result would not be affected by the initial composition of seed

1 Buffer abbreviations are given in the section on epidote stability as a function of f_{O_2}.

Table 1. Chemical analyses, optical data, and X-ray data for epidote minerals

Locality	Timmons Ontario	Baja Calif.[a]	Baja Calif.	Plumas Co. Calif.	Calumet Colo.	Greenhorn Mtns., Calif.	Unknown
% Pistacite[b]	$Ps_{11.6}$	$Ps_{13.0}$	$Ps_{17.7}$	$Ps_{24.7}$	$Ps_{26.2}$	$Ps_{27.5}$	$Ps_{33.3}$
SiO_2	38.77	38.18	37.95	37.62	37.63	36.95	36.83
Al_2O_3	28.97	28.66	26.48	23.96	23.42	22.99	20.96
Fe_2O_3[c]	6.05	6.61	8.92	12.40	13.01	13.88	16.23
TiO_2	0.14	n.d.	0.11	0.16	0.36	0.11	0.07
CaO	23.89	24.11	23.42	23.17	23.33	22.53	23.00
MgO	0.03	0.16	0.03	0.03	0.09	0.03	0.10
MnO	0.11	n.d.	0.28	0.22	0.10	0.44	0.18
FeO	n.d.	0.42	n.d.	n.d.	n.d.	n.d.	n.d.
Total[aa]	97.96	98.14	97.19	97.56	97.94	96.93	97.37
Structural formula based on 8 metal ions							
Si	3.002	2.955	2.997	2.999	2.995	2.982	2.984
Al	3.00	0.045 3.00	0.003 3.00	0.001 3.00	0.005 3.00	0.018 3.00	0.016 3.00
Al	2.644	2.570	2.461	2.250	2.192	2.169	1.985
Fe^{+3}	0.348 3.00	0.385 2.96	0.530 3.00	0.740 3.00	0.779 2.99	0.824 3.00	0.990 2.98
Ti	0.008		0.006	0.010	0.022	0.007	0.004
Ca	1.982	1.999	1.981	1.979	1.990	1.948	1.996
Mg	0.003	0.018	0.003	0.003	0.011	0.003	0.012
Mn	0.007 2.00	2.04	0.018 2.00	0.015 2.00	0.007 2.01	0.030 2.00	0.012 2.02
Fe^{+2}	0.005	0.027	0.000	0.004	0.000	0.019	0.000
α[bb]	1.712	1.713	1.721	1.728	1.729	1.730	1.741
β	1.718	1.720	1.732	1.746	1.751	1.753	1.771
γ	1.724	1.727	1.743	1.763	1.768	1.772	1.790
$2V_\gamma$° (calc)	90	90	90	93	99	97	105
a, Å[cc]	8.874	8.878	8.876	8.888	8.893	8.903	8.894
b, Å	5.602	5.600	5.613	5.630	5.631	5.617	5.651
c, Å	10.147	10.145	10.160	10.151	10.145	10.169	10.161
β, °	115.45	115.44	115.40	115.34	115.34	115.50	115.35
V, Å^3	455.45	455.48	457.24	459.10	459.20	458.96	461.58

[a] See also Holdaway (1966).

[b] Calculated as octahedral Fe/Al + Fe.

[c] Total Fe as Fe_2O_3.

[aa] Water analysis for epidotes averages 1.86 (Deer, Howie, and Zussman, 1962).

[bb] Indices are ± 0.002.

[cc] X-ray data obtained by averaging between 7 and 10 spacings from two slow scans of each mineral on a General Electric XRD-6 spectrometer using silicon a san internal standard. Lattice parameters were refined using the computer program of Burnham (1962). Average errors generated by the computer refinement are a 0.004, b 0.002, c 0.005, β 0.04, V 0.51.

grains. A determinative curve of β against composition was plotted using available analytical data (Fig. 1). Below Ps_{29} a linear least squares fit gives $Ps = 517.5\ \beta - 877.7$. Of the values plotted, 87% fall within ± 2 mol% of the predicted value. Above Ps_{29} curvature in the plot probably results from the fact that at these compositions much of the Fe is entering the M(1) site as discussed in a later section of this report. Fig. 1 agrees satisfactorily with a similar plot by Strens (1965).

The cell dimensions for epidotes (Table 1) are in reasonable agreement with results of Myer (1965, 1966), but on the average they are about 1 part in 2000 lower than Myer's curves. Each

Table 2. Chemical analyses, optical data, and X-ray data for grossularite-andradite minerals

Locality	Chihuahua Mexico[a]	Unknown	Klamath Mtns. Calif.	Boulder Batholith Mont.	Willsboro N.Y.
% Andradite[b]	$And_{12.8}$	$And_{21.3}$	$And_{33.3}$	$And_{41.0}$	$And_{54.8}$
SiO_2	39.13	38.30	37.99	37.53	37.38
Al_2O_3	19.35	16.85	13.95	12.45	9.26
Fe_2O_3[c]	4.40	8.58	11.67	14.28	18.13
TiO_2	0.00	0.64	0.77	0.16	0.78
CaO	35.67	34.14	33.76	33.80	33.57
MgO	0.76	0.08	0.44	0.15	0.30
MnO	0.09	0.69	0.25	0.58	0.11
FeO	0.13	n.d.	n.d.	n.d.	n.d.
Total	99.53	99.28	99.83	98.95	99.53
Structural formula based on 8 metal ions					
Si	2.985 } 3.00	2.993 } 3.00	3.015 } 3.01	3.003 } 3.00	3.020 } 3.02
Al	0.015 }	0.007 }			
Al	1.724 }	1.545 }	1.304 }	1.174 }	0.882 }
Fe^{+3}	0.253 } 1.98	0.418 } 2.00	0.650 } 2.00	0.816 } 2.00	1.071 } 2.00
Ti	0.000 }	0.037 }	0.046 }	0.010 }	0.047 }
Ca	2.915 }	2.858 }	2.869 }	2.897 }	2.905 }
Mg	0.086 }	0.009 }	0.052 }	0.018 }	0.036 }
Mn	0.006 } 3.02	0.047 } 3.00	0.017 } 2.99	0.039 } 3.00	0.008 } 2.98
Fe^{+2}	0.008 }	0.086 }	0.047 }	0.042 }	0.031 }
Grossularite	83.9	72.6	61.3	55.4	41.6
Andradite	12.8	20.9	32.5	40.8	53.6
Ti Andradite	0	1.8	2.3	0.5	2.3
Almandine	0.3	2.9	1.6	1.4	1.0
Pyrope	2.8	0.3	1.7	0.6	1.2
Spessartite	0.2	1.5	0.6	1.3	0.3
N[aa]	1.750	1.770	1.791	1.800	1.822
a, Å[bb]	11.875	11.889	11.914	11.929	11.965
V, Å	1674.56	1680.49	1691.11	1697.51	1712.92

[a] See also Holdaway (1966).

[b] Calculated as octahedral Fe/Al + Fe.

[c] Total Fe as Fe_2O_3.

[aa] Indices are ± 0.002.

[bb] X-ray data obtained by averaging four slow scans of (642) for each mineral on a General Electric XRD-6 spectrometer using silicon as an internal standard. Estimated error in a 0.003.

garnet cell parameter is in good agreement with a value of a calculated from the data of Huckenholz and Yoder (1971) for andradite and Skinner (1956) for the other end members.

Anorthite for the experiments is from Miakejima, Japan. A chemical analysis gives SiO_2—44.5%, Al_2O_3—35.2%, Fe_2O_3—0.52%, CaO—19.4%, Na_2O—0.47%, K_2O—0.00%. The composition is thus $An_{96}Ab_4Or_0$. Hematite and magnetite from unknown localities were qualitatively analyzed by atomic absorption and shown to have no significant impurities. White wollastonite from Willsboro, New York, was used for grossularite-andradite experiments. Two unanalyzed garnets were used in some experiments. These had approximate compositions of And_{82} and And_{100} as determined from refractive index and unit cell determinations (Hucken-

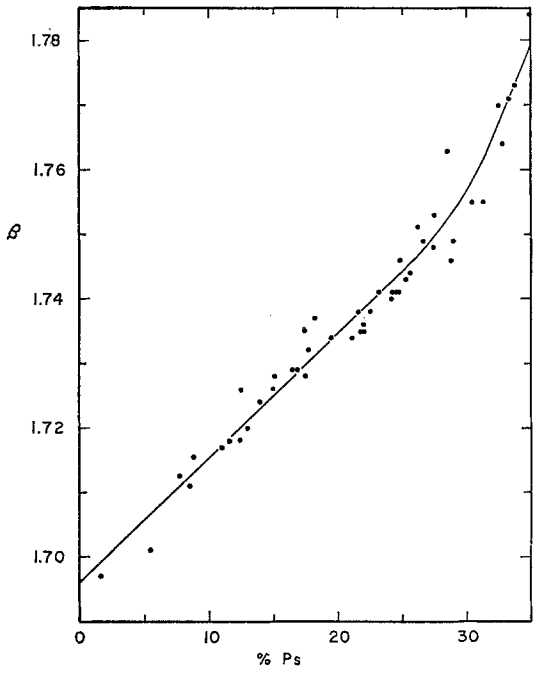

Fig. 1. Dependence of β on composition for Al-Fe epidotes. Points plotted represent the analyses of Deer *et al.* (1962), Myer (1965, 1966) and this report (Table 1). The solid line predicts epidote composition from β within ± 2 mol% for most cases

holz and Yoder, 1971). A zoisite-clinozoisite mixture with a bulk composition of $Ps_{3.5}$ (determined by iron analysis) was also used in one run. Quartz from Hot Springs, Arkansas and synthetic corundum from Union Carbide comprised the remainder of the starting materials for epidote reactions. For a few experiments, finely powdered reagent hematite and calcite or portlandite were used in addition to minerals identified above.

Experimental Procedure

Experiments on epidote stability were conducted with cold-seal pressure vessels using water as the pressure medium. Temperatures given are believed accurate to $\pm 5°$ C while pressures are $\pm 1.5\%$.

Three experimental techniques were used successfully. (1) Equal amounts of products and reactants were mixed, and reaction direction was detected by comparing X-ray peak heights for product and reactant minerals. (2) The experimental charge consisted of reactants seeded with small amounts of products. Reaction was detected by study of run products with the petrographic microscope. (3) Crystals of corundum were used as a reaction monitor, surrounded by powder of the remaining reaction participants. Direction of reaction was indicated by weight change of the corundum crystal during the run (Holdaway, 1966, 1971).

Experimental charges were buffered with respect to oxygen fugacity with oxide mixtures (Eugster and Wones, 1962). The experimental capsule was composed of $Ag_{70}Pd_{30}$ or rarely silver or platinum, while the outer capsule was composed of silver or, when needed, gold.

Whenever the nature of the experiments required a knowledge of the composition of solid solution run products, this was accomplished with the use of index of refraction and/or X-ray diffraction measurements. For epidote Fig. 1 was used to determine composition from a measurement of β. For run products in which epidote growth was large relative to the initial amount of seed mineral present, composition was also determined by measurement of the (020) X-ray reflection (Myer, 1966). In such cases the agreement between the two methods was good, and the reported value is an average of the compositions from both methods.

Although natural garnets exhibit solid solution with six important end members, Ti andradite, spessartite, and pyrope may be eliminated from consideration in this report because

Ti, Mn, and Mg were always present in no more than trace amounts. The run products were thus solid solutions of grossularite, andradite, and almandine, assuming that the hypothetical skiagite molecule $Fe_3^{+2}Fe_2^{+3}Si_3O_{12}$ is not involved. Garnet composition was determined from measurement of refractive index and a in run products which showed substantial increase in garnet. The unit cell dimension was determined from slow scans of (642) using an internal standard of quartz or silicon. The cell dimensions and refractive indices of the end members determined by Skinner (1956) for grossularite and Huckenholz and Yoder (1971) for andradite ($n = 1.887$, $a = 12.059$) were used, and it was assumed that the variations in a and N are a linear function of end member proportions.

Determination of garnet composition was further simplified under oxidizing conditions. Use of the above method showed that almandine content of run product garnet was never more than 3% with the MH buffer. Thus where abundant growth of garnet occurred a measurement of refractive index *or* cell dimension sufficed to determine the grossularite-andradite composition under conditions of the more oxidizing CT buffer. Under MH buffer conditions it is reasonable to assume that almandine component is negligible for low-iron garnets such as those produced by clinozoisite breakdown. The values given for epidote and garnet compositions participating in reactions are believed to be accurate to ± 2 or 3 mol% except where special problems are noted.

Fe-Al Partitioning between Garnet and Epidote

Clinozoisite and epidote decomposition reactions always produce grandite garnet. The partitioning of ferric iron and aluminum between epidote and garnet must be known before epidote reactions can be thoroughly understood. The experiments described below were carried out at 3000 bars H_2O pressure between 645 and 655° C with a MH buffer, Ag-Pd charge capsules, and 28 to 47 day runs.

Each experimental run consisted of two capsules containing 25 mg of garnet of known composition, 5 mg of quartz or corundum and 34 mg of water. One of the capsules contained 0.6 mg of an epidote more aluminum-rich than expected equilibrium epidote, and the other capsule contained 0.6 mg of an epidote more iron-rich than the expected equilibrium composition. During the experiment the epidote seeds showed new crystal faces and the rims changed composition. Measurement of refractive indices of the rim portions showed that in each pair of capsules with the same garnet composition, the epidote seeds changed to refractive indices within 0.001 of each other.

Equilibrium epidote compositions were determined with the aid of Fig. 1; these were plotted against garnet composition as analyzed (Table 2) in Fig. 2. Checks of run product garnet composition by refractive index and X-ray diffraction showed that changes from the analyzed composition during experiments were less than 1 mol %. The epidote and garnet compositions from several reactions studied, discussed in later sections (Table 3, 4), are also plotted.

The curve given in Fig. 2 is based on a empirical treatment of all the experimental data under MH buffer conditions and will be used here as an aid to determine compositions of epidote and garnet involved in divariant reactions. The estimated maximum error of this curve is ± 3 mol %.

The divariant breakdown of clinozoisite with quartz to anorthite and garnet studied by Holdaway (1966) made use of clinozoisite (Ps_{13}) and grossularite ($And_{12.8}$). From the partition curve it can be seen that the equilibrium forward reaction was $Ps_{13} \rightarrow And_{22}$ while the reserve reaction was $And_{12.8} \rightarrow Ps_7$. The reaction best represented by the equilibrium curve is the average of these two, or $Ps_{10} \rightarrow$

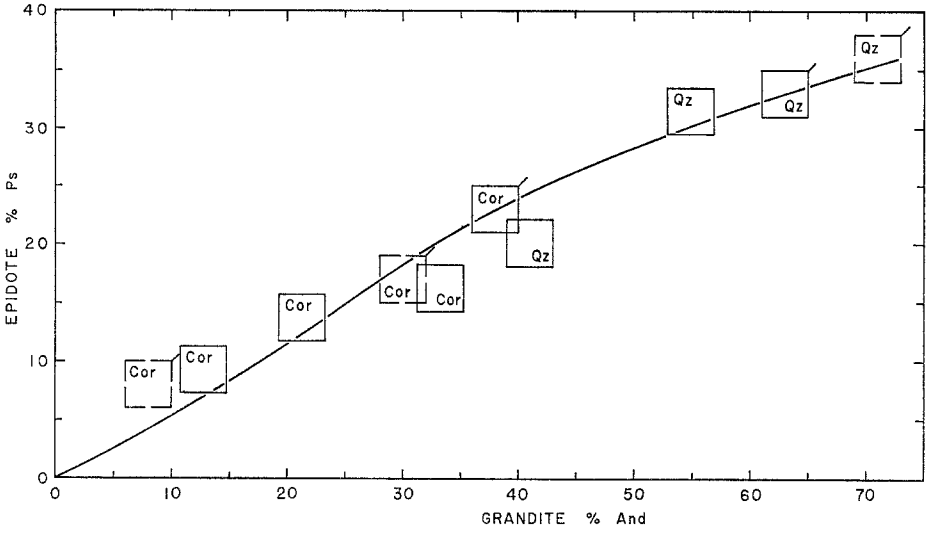

Fig. 2. Diagram to show partitioning of Fe^{+3} between coexisting garnet and epidote based on experimental results. Boxes bounded by solid lines: MH buffer; by dashed lines: other buffers. Boxes without flags: garnet and epidote equilibrated together at 640°, 3000 bars; boxes with flags: epidote and garnet are equilibrium reactant and product (Tables 3, 4, reactions 1–4). Solid partition curve is based on analysis of MH buffer results (see section on calculated phase relations). *Qz* quartz present; *Cor* corundum present

And_{17}. This procedure will also be used to determine epidote and garnet compositions for the divariant silica-deficient clinozoisite reaction.

A difference of 6 mol % in epidote composition between the forward and reverse reactions as suggested above should produce an offset between the weight gain and weight loss curves for clinozoisite-quartz stability (Holdaway, 1966, p. 656). The fact that such an offset was not found in that study was used as an argument that Ps_{13} was approximately stable with $And_{12.8}$. Assuming the validity of the partitioning curve, the absence of such offsets may be due to a tendency for the garnet and epidote to equilibrate by ion exchange in the surface layers as they start to react. The averaging of the forward and reverse reactions should still provide the best representation of the reaction studied.

Epidote Stability as a Function of Oxygen Fugacity at 3000 Bars

Experimental Procedure

Experiments were conducted on epidote stability with several oxygen buffers at a total pressure of 3000 bars for durations of 14 to 28 days. The following buffers were used: Cuprite-Tenorite (CT), Magnetite-Hematite (MH), Manganosite-Hausmanite (MHa), and Nickel-Bunsenite (NB). Huebner (1971) gives a good recent summary of the use of oxygen buffers. All buffers were X-rayed at the end of the run to be sure the complete buffer assemblage remained.

Experimental results are summarized in Table 3. For each buffer, the reaction being observed was the univariant breakdown of the most iron-rich epidote stable on that buffer curve. Because the limiting epidote composition is a function of

Table 3. Experimental results on epidote stability as a function of f_{O_2} $P = 3000$ bars[a]

Run	T °C	Starting materials	Products
A. Cuprite-tenorite buffer			
257	715	$Ps_{33.3}$ + Qz + And_{32} + An + Hem	$And_{71}Gr_{29}$ + Qz + An + Hem (Ps_{34})
327	752[b]	$Ps_{33.3}$ + Qz + *And_{32}*	$And_{69}Gr_{31}$ + Qz + An + Hem (Ep)
332	695	Run 327	Ps_{36} + Qz ($And_{71}Gr_{29}$ + An + Hem)
338	709	Run 327	Ps_{36} + Qz ($And_{73}Gr_{27}$ + An + Hem) ?
345	728	Run 327	$And_{72}Gr_{28}$ + Qz + An + Hem (Ep)
B. Magnetite-hematite buffer			
(Experiments for silica-excess reaction reported in Table 4, Fig. 5)			
399	723	$Ps_{33.3}$ + Cor + *$And_{54.8}$* + *An* + Hem	$And_{39}Gr_{61}$[c] + Cor + An + Hem + Mag (Ep)
407	690	Run 399 + *$Ps_{24.7}$*	Ep + Cor (Ga + An + Mag) ?
423	682	Run 407	Ps_{23} + Cor (Ga + An + Mag)
604	701	$Ps_{24.7}$ + Cor + *And_{41}* + An + Hem	$And_{38}Gr_{60}Alm_2$ + Cor + An + Mag (Ep)
C. Manganosite-hausmanite buffer			
353	727[aa]	$Ps_{33.3}$	$And_{39}Gr_{50}Alm_{11}$ + An + Mag + Hd
355A	639	Run 353 + Qz + *$Ps_{17.7}$*	Ga + Qz + An + Mag
355B	628	Run 353 + Cor + *$Ps_{17.7}$*	Ps_{17} + Cor (Ga + An + Mag)
363	640	Run 353 + Cor + *$Ps_{24.7}$* + Mag	Ps_{17} + Cor (Ga + An + Mag)
364A	696	$Ps_{24.7}$ + Cor + An + Mag + *Run 353*	$And_{30}Gr_{63}Alm_7$ + Cor + An + Mag (Ep)
364B	690	$Ps_{17.7}$ + Cor + An + Mag + *Run 353*	Ga + Cor + An + Mag (Ep)
373	683	$Ps_{17.7}$ + *Cor* + *Run 353*	Ep + Cor (Ga)
374	670	Run 353 + Cor + *Ps_{13}* + Mag	Ps_{17} + Cor (Ga + An + Mag)
D. Nickel-bunsenite buffer			
342	670[bb]	$Ps_{17.7}$ + $And_{21.3}$	$And_{18}Gr_{72}Alm_{10}$ + An + Hc (Ep)
385	691	Ps_{13} + Cor + *Run 342*	$And_{11}Gr_{85}Alm_4$ + Cor + An + Hc
405	656	$Ps_{11.6}$ + *Cor* + $Hc_{85}Mag_{15}$ + *Run 385*	$And_4Gr_{77}Alm_{19}$ + Cor + An + $Hc_{86}Mag_{14}$ (Ep)
412	642	Run 385 + Cor + *$Ps_{3.5}$*[cc] + $Hc_{85}Mag_{15}$	Ps_8 + Cor (Ga + An + Hc)

[a] Mineral abbreviations: Ep = Epidote; Ps = epidote composition; Ga = garnet; And, Gr, Alm = garnet composition in terms of andradite, grossularite, almandine; An = anorthite; Qz = quartz; Cor = corundum; Hem = hematite; Mag = magnetite; Hc = hercinite; Hc, Mag = hercynite composition in terms of hercynite, magnetite; Hd = hedenbergite; Run 327 = products of run 327; *And_{85}* = 1–5% of starting materials; (Ps_{34}) = present in products but texture and amounts shows it to be unstable. Solid solution compositions in mol.%.

[b] $P = 1930$ bars.

[c] Based on refractive index only.

[aa] $P = 2068$ bars.

[bb] $P = 2896$ bars.

[cc] Mixture of clinozoisite and zoisite.

f_{O_2}, the stability curves shown on Fig. 3 apply to changing epidote and garnet compositions. The experimental procedure involved the following steps: (1) An epidote more iron-rich than the expected equilibrium composition was subjected to conditions well above the dehydration temperature, commonly at pressures below 3000 bars. This provided a first estimate of the decomposition products and garnet composition. (2) Using the products of step 1 seeded with epidote, the reac tion was reversed at a lower temperature at 3000 bars pressure and the stable epidote composition was determined. (3) Using either products of earlier runs or

natural minerals of the correct composition the equilibrium conditions and reaction participants were more precisely determined with more closely spaced runs.

Several difficulties were encountered. Reactions rarely went to completion. In many cases it was necessary to study the refractory minerals with the petrographic microscope to observe overgrowths and crystal faces indicating stability, or corrosion and reduction in amount indicating instability. Phases were identified by X-ray diffraction in some cases, but most often by petrographic microscope. Experimental products were always reground in an agate mortar before being rerun, so that new growth could be recognized.

A second problem involved the nature of the other phases participating in the reaction. The epidote breakdown phases consisted of anorthite, grossularite-andradite garnet, one (or rarely two) iron oxides, and quartz or corundum. Because the amount of quartz or corundum involved in the reactions was small, and because the initial epidote starting composition was not the equilibrium epidote composition it was not normally possible to tell directly whether quartz or corundum was a product. This problem was solved indirectly by experimenting with a quartz-rich and a corundum-rich system in some cases, and by balancing the equilibrium reaction.

Another difficulty arose with NB buffered experiments. Both Ag and Ag-Pd tubing are unsatisfactory with the NB buffer because alloying occurs and most capsules fail before completion of the run. Therefore Pt capsules were used. The experimental charge has a tendency to lose iron to the Pt capsule walls. The most satisfactory runs with NB buffer were those containing initial excess hercynite. Hercynite for these runs was synthesized with a composition of $Hc_{85}Mag_{15}$ such that it would be stable with corundum at the NB buffer (Turnock and Eugster, 1962, p. 549).

Interpretation of Results

Under silica-deficient conditions of the MH buffer hematite was only rarely observed as a reaction product. Apparently, corundum stabilized magnetite relative to hematite under MH buffer conditions. This was also observed by Turnock and Eugster (1962).

The limiting conditions of reversal for epidote stability with the various buffers are plotted on Fig. 3 to show the stability field of epidote as a function of f_{O_2} at 3000 bars. The solid lines bound the epidote stability field. The epidote stability field is bounded by an upper segment for which quartz is a product of epidote decomposition and a lower segment for which corundum is a product of epidote decomposition. The upper dashed segment represents conditions at which epidote reacts with corundum at lower temperatures than it breaks down alone; the lower dashed segment represents conditions at which epidote reacts with quartz at lower temperatures than it breaks down alone. Thus the epidote field is bounded by an excess-silica line and an excess-corundum line, and each line marks the upper boundary of epidote stability over a range of conditions. The dashed portions of both lines are drawn schematically to fit the available data.

Balanced reactions for epidote decomposition under four buffer conditions are given below. In interpreting the data of Table 3 only run products which grew in amount were used. Except for the NB buffered runs discussed above, runs which showed sufficient reaction for composition measurements appeared to be relatively insensitive in composition of the stable phases to starting amounts and compositions. Wherever X-ray and optical methods were used together they gave con-

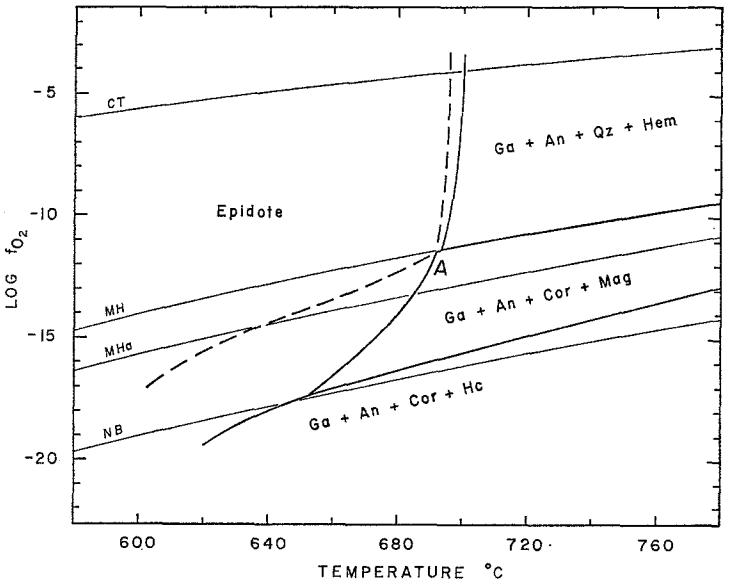

Fig. 3. Stability relations of epidote at 3000 bars as a function of f_{O_2} and temperature. Buffer curves are taken from Huebner (1971), except for CT which was calculated from data of Robie and Waldbaum (1968). Solid line represents stability of epidote, upper dashed line represents approximate stability of epidote-corundum, lower dashed line represents approximate stability of epidote-quartz. Abbreviations, given in Table 3, show products and reactants for epidote decomposition reactions 1–4. Note that where the two lines cross at A, corundum and quartz do not coexist because the system changes composition from about Ps_{32} with quartz to about Ps_{22} with corundum. A narrow field of Ga + An + Qz + Mag below the MH buffer is not shown. Hercynite-magnetite boundary from Turnock and Eugster (1962)

sistent results suggesting that the average and final composition were the same within the limits of error.

The Fe^{+3} content of anorthite in equilibrium with grandite is an unknown quantity which has a small effect on the various relations discussed in this report. K_D for partitioning of Fe^{+3} and Al between anorthite and garnet, defined as $(X^A_{Fe}X^G_{Al})/(X^A_{Al}X^G_{Fe})$ is assumed to be 0.01 at all temperatures. This value gives maximum Fe contents consistent with anorthite analyses. Anorthite compositions given in reactions 1–4 and elsewhere in this report are based on this assumed distribution. The effect of Fe^{+2} replacing Ca in anorthite and epidote is neglected because it is difficult to estimate and probably small under all but the most reducing conditions.

CT $4\ Ca_2(Fe_{0.36}Al_{0.64})_3Si_3O_{12}(OH) \rightleftarrows$
$1.5\ Ca_3(Fe_{0.71}Al_{0.29})_2Si_3O_{12} + 3.5\ CaAl_{1.95}Fe_{0.05}Si_2O_8$ (1)
$+ 0.5\ SiO_2 + Fe_2O_3 + 2\ H_2O$

MH $4\ Ca_2(Fe_{0.33}Al_{0.67})_3Si_3O_{12}(OH) \rightleftarrows$
$1.54\ (Ca_{0.97}Fe_{0.03})_3(Fe_{0.63}Al_{0.37})_2Si_3O_{12} + 3.51\ CaAl_{1.97}Fe_{0.03}Si_2O_8$ (2)
$+ 0.36\ SiO_2 + 0.59\ Fe_3O_4$[2] $+ 0.37\ O_2 + 2\ H_2O$

2 Or $0.89\ Fe_2O_3 + 0.07\ O_2$.

MHa $4\ Ca_2(Fe_{0.17}Al_{0.83})_3Si_3O_{12}(OH) \rightleftarrows$
$1.56\ (Ca_{0.93}Fe_{0.07})_3(Fe_{0.30}Al_{0.70})_2Si_3O_{12} + 3.66\ CaAl_{1.99}Fe_{0.01}Si_2O_8$ (3)
$+ 0.25\ Al_2O_3 + 0.25\ Fe_3O_4 + 0.29\ O_2 + 2\ H_2O$

NB $4\ Ca_2(Fe_{0.08}Al_{0.92})_3Si_3O_{12}(OH) \rightleftarrows$
$1.71\ (Ca_{0.89}Fe_{0.11})_3(Fe_{0.08}Al_{0.92})_2Si_3O_{12} + 3.44\ CaAl_2Si_2O_8$ (4)
$+ 0.43\ Al_2O_3 + 0.09\ Fe(Al_{0.86}Fe_{0.14})_2O_4 + 0.33\ O_2 + 2\ H_2O.$

These reactions show that as f_{O_2} is reduced, epidote becomes more aluminous, garnet increases in grossularite component and, to some extent, almandine. As corundum becomes a stable product, epidote and garnet composition abruptly become more aluminous. The iron oxide changes from hematite to magnetite to hercynite. Comparison of the epidote and garnet compositions with Fig. 2 shows that if possible small temperature effects are ignored the distribution coefficient for Fe^{+3} and Al between epidote and garnet is not significantly affected by f_{O_2}

Where the excess-silica and excess-corundum curves cross (Fig. 3) all epidote compositions between about Ps_{22} and Ps_{32} (see Table 3B and reaction 2) decompose alone at a single temperature of 691° C, and neither quartz nor corundum is involved in the reaction. At other oxygen fugacities in the absence of quartz and corundum, epidote of any composition between that stable on the excess-silica curve and that stable on the excess-corundum curve fractionally decomposes at temperatures ranging between the two curves. This must happen with quartz and corundum absent for as soon as quartz or corundum is present, then the limiting composition of the epidote and its breakdown curve are determined by one of the two curves given in Fig. 3.

In exploratory excess-silica runs under reducing conditions (NB buffer) hedenbergite appeared in place of hercynite. Excess-silica reactions are difficult to study under reducing conditions because the grossularite garnets tend to react with quartz not far above the epidote breakdown conditions, and stable or metastable wollastonite forms readily from epidote + quartz reactions.

In a recent abstract Liou (1972) reports results of experiments on epidote stability with various oxygen buffers. He apparently used epidote composition with excess silica. Most of his results cannot be compared directly with those reported here because excess silica lowers the stability of epidote minerals under reducing conditions. Also, the effect of using epidote composition with the fayalite-magnetite-quartz buffer, where clinozoisite is probably the stable phase, adds excess Fe to the system and may further lower the decomposition temperature. Under these conditions the reaction studied by Liou may have been: clinozoisite + hedenbergite $\rightleftharpoons$ grossularite-almandine + quartz + anorthite.

Pressure-Temperature Decomposition Curves for Epidote Minerals

To date three stability curves for Fe-Al epidote minerals have been determined in the writer's laboratory, all under conditions of the MH buffer. These are (1) the stability of epidote, (2) the stability of clinozoisite, and (3) the stability of clinozoisite + quartz (Holdaway, 1966). With the exception of the oxygen buffer technique discussed earlier, these studies have been approached in somewhat differing ways.

Stability of Epidote

Under conditions of the MH buffer epidote undergoes a univariant breakdown to garnet, anorthite, hematite, and quartz (reaction 2). This reaction was studied as a function of pressure and temperature using two experimental approaches. Epidote ($Ps_{33.3}$) with quartz was the initial starting material. From this starting material the breakdown assemblage was prepared in a 15 day run at 2068 bars and 750° C.

One experimental method utilized X-ray diffraction to determine the direction of reaction. Equal amounts of products and reactants were ground in an agate mortar and subjected to experimental conditions with the MH buffer for between 21 and 35 days, depending on the pressure. Run products were briefly ground again, sedimented on a glass slide, and X-rayed at a scanning speed of 0.4° per minute. For each run product as well as the initial mix the peak height ratios of garnet (420) to epidote ($11\bar{3}$) and of anorthite (220) to epidote ($11\bar{3}$) were measured. For the great majority of runs these ratios were either both above or both below the ratios for the standard. Problems related to preferred orientation in samples did not appear because the method of preparation was kept constant and two of the minerals, epidote and garnet, do not have well-developed cleavages. The X-ray slides for which the ratios had increased were shades of gray in color, while those for which the ratios had decreased were shades of pistachio green. The runs for which both peak height ratios increased relative to the standard were interpreted as indicating epidote instability while those for which both ratios decreased were interpreted as indicating epidote stability. The extent of reaction for observable change was estimated at 15%.

The second method involved use of the petrographic microscope to indicate reaction direction. The experimental charge consisted of 97% of the assemblage assumed to be unstable and 3% of the assemblage assumed to be stable. After 21 to 35 days at the experimental conditions, the charge was examined. Overgrowths and crystal faces on the seed mineral garnet or epidote were taken to indicate stability, while corrosion or disappearance of seeds was indicative of instability of the seed mineral assemblage.

The two experimental methods show excellent agreement (Fig. 5) and serve to delineate the stability field of epidote under the most oxidizing conditions likely to occur in nature. Compositions of epidote and garnet applicable to this reaction were averaged from the experimental data given in Table 4. The table also shows that there is no recognizable change in composition of epidote or garnet between 1000 and 3000 bars along the stability curve.

Stability of Clinozoisite

Under oxidizing conditions clinozoisite breaks down along a divariant curve to more iron-rich compositions of epidote along with grossularitic garnet, anorthite, and corundum. The reaction is the silica-poor analogue of the clinozoisite-quartz reaction (Holdaway, 1966). Attempts were made to study these divariant reactions directly by equilibrating garnet and epidote with anorthite and corundum or anorthite and quartz, but they were unsuccessful, probably because two solid solution minerals had to change composition while each remained stable as a phase. The alternative approach of using specific compositions of clinozoisite and garnet to determine a single curve for clinozoisite stability was successful.

The clinozosite reaction was studied with the MH buffer using a single crystal of synthetic corundum as a reaction minotor (Holdaway, 1966, 1971). For each run a carefully ground cylindrical corundum crystal (between 40 and 80 mg) was accurately weighed and immersed in 50 mg of a powder containing equal weights of clinozoisite ($Ps_{11.6}$), grossularite ($And_{12.8}$), and anorthite, along with 38 mg of water. Run times were 30 days at 1034 bars and 16 days at 2068 and 3102 bars. Each crystal was reweighed after the experimental run, and weight

Table 4. Composition of epidote and garnet in the univariant breakdown reaction of epidote with the magnetite-hematite buffer[a]

Run	T °C	P bars	Composition of stable epidote or garnet
278A	678	3102	$Ps_{34.2}$
281A	642	2068	$Ps_{33.0}$
283A	691	3102	$Ps_{32.8}$
293A	568	1034	$Ps_{33.3}$
271	750	2068	$And_{62.4}Gr_{34.9}Alm_{2.7}$
277B	711	3102	$And_{63.4}Gr_{34.5}Alm_{2.1}$
289B	594	1034	$And_{63.3}Gr_{33.4}Alm_{3.3}$

[a] Mineral abbreviations as for Table 3.

change was determined to an accuracy of ± 4 μg (Holdaway, 1971, p. 105). Weight gains were interpreted as indicating clinozoisite instability, producing corundum, and weight losses were used to indicate clinozoisite stability.

Experimental results at the three pressures are presented in Fig. 4. The corundum exhibits a small initial weight loss while the equilibrium fluid is forming. The extent of this loss is indicated by one or two day runs at each pressure. Comparable weight losses have been observed in runs as short as two hours. Although the cause of this loss is uncertain, it may be solution of a disordered surface layer on the synthetic corundum. For a given pressure, the point at which the long term weight change curve crosses the short term line is the condition at which the weight change is the same regardless of the length of the run. This temperature is assumed to be the equilibrium condition. The equilibrium curve based on these temperatures (Fig. 5) lies between the clinozoisite-quartz and epidote equilibrium boundaries. From the epidote-garnet partitioning curve (Fig. 2) it can be seen that the equilibrium garnet produced during the reaction of $Ps_{11.6}$ is And_{20}. In the reverse direction the $And_{12.8}$ must produce Ps_7. Thus the curve in Fig. 5 best represents an average of these two reactions of $Ps_9 \rightarrow And_{16}$. For a 1 mol % change in epidote composition the reaction is:

$$\begin{aligned} &38\ 2/3\ Ca_2(Al_{0.91}Fe_{0.09})_3Si_3O_{12}(OH) \rightleftarrows \\ &32\ 2/3\ Ca_2(Al_{0.90}Fe_{0.10})_3Si_3O_{12}(OH) \\ &+ 2\ Ca_3(Al_{0.84}Fe_{0.16})_2Si_3O_{12} + 6\ CaAl_2Si_2O_8 + Al_2O_3 + 3\ H_2O. \end{aligned} \tag{5}$$

Stability of Clinozoisite-Quartz

The equilibrium curve for clinozoisite-quartz stability (Holdaway, 1966) is shown in Fig. 5 corrected for a 4° C error in thermocouple calibration. The balanced reaction for 1 mol % change in epidote composition is given below.

$$\begin{aligned} &32\ 2/3\ Ca_2(Al_{0.90}Fe_{0.10})_3Si_3O_{12}(OH) + SiO_2 \rightleftarrows \\ &28\ 2/3\ Ca_2(Al_{0.89}Fe_{0.11})_3Si_3O_{12}(OH) \\ &+ Ca_3(Al_{0.83}Fe_{0.17})_2Si_3O_{12} + 5\ CaAl_2Si_2O_8 + 2\ H_2O. \end{aligned} \tag{6}$$

Each of the three stability curves studied has an estimated maximum error of ± 15° C.

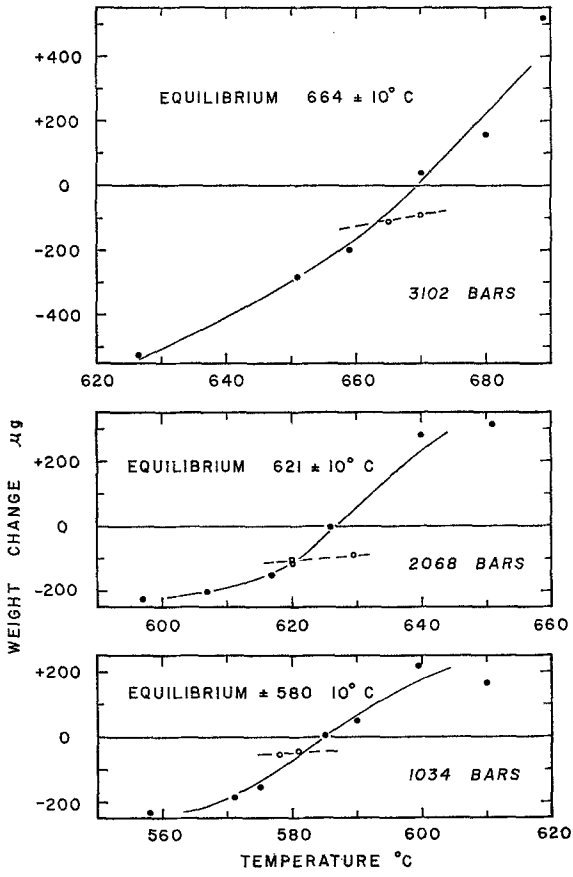

Fig. 4. Results of corundum crystal experiments in powder of anorthite, $Ps_{11.6}$, and $And_{12.8}$. Solid symbols: run times of 16 or 30 days; open symbols: run times of 1 or 2 days. See text for further explanation

Ideality of the Grossularite-Andradite Solid Solution

In order to use the experimental results to calculate thermodynamic data for epidote and temperature-composition diagrams for the divariant reaction of epidote to garnet-bearing assemblages, it would be useful to know whether the grossularite-andradite solid solution is ideal. Two types of experiments were conducted on grandite breakdown equilibria. These experiments demonstrate that the solid solution is nearly ideal, and provide an approximate temperature-composition diagram for grandite-quartz stability under oxidizing conditions.

In the presence of quartz, grossularite decomposes according to the reaction

$$Ca_3Al_2Si_3O_{12} + SiO_2 \rightleftarrows CaAl_2Si_2O_8 + 2\,CaSiO_3. \quad (7)$$

Under oxidizing conditions addition of andradite molecule produces a divariant reaction in which garnet and quartz react to produce anorthite, wollastonite, and progressively more andradite-rich garnet as temperature increases. In the discussion which follows, anorthite and grandite are assumed to be ideal ionic solutions. On the basis of this assumption entropy change for reaction 7 (ΔS_{Gr}) may be calculated from the two series of experiments and the results compared

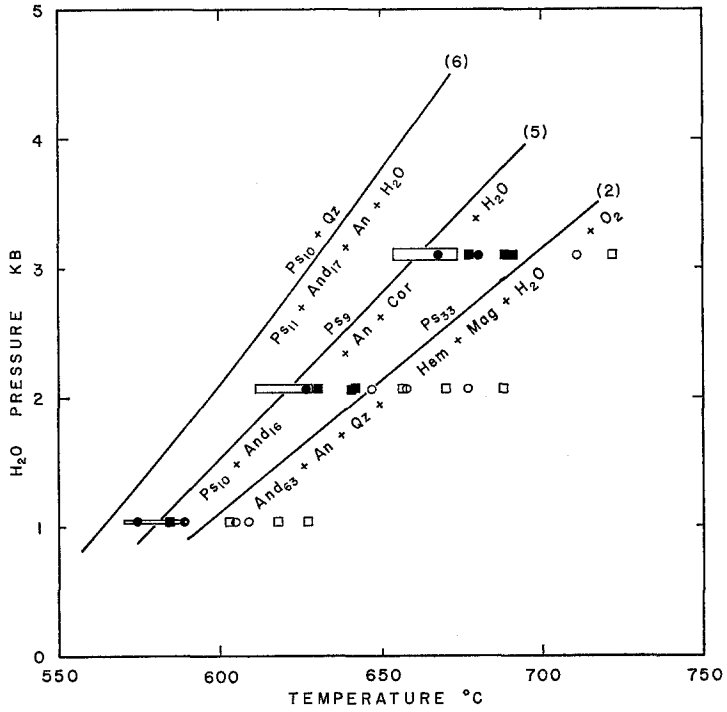

Fig. 5. Pressure-temperature diagrams for reactions 2, 5 and 6 under conditions of the MH buffer. Abbreviations as for Table 3. Reaction 6 is from Holdaway (1966). Rectangles for reaction 5 represent limits of error for the equilibrium condition, based on Fig. 4. For reaction 2 closed symbols: epidote stability; open symbols: instability; dots: X-ray determination of stability; squares: seeding runs

with ΔS_{Gr} based on the slope of reaction 7. Agreement obtained by the two methods is taken as an approximate indication of ideality. One must also assume that ΔS_{Gr} is independent of temperature, a reasonable assumption for solid-solid reactions.

Consider a temperature T at which some garnet composition X^G_{Al} and anorthite composition X^A_{Al} are in equilibrium with wollastonite and quartz[3]. At this temperature the free energy of reaction 7 may be given by either of two expressions: $-(T-T_{Gr})\Delta S_{Gr}$ or $-RT \ln (X^{A^2}_{Al}/X^{G^2}_{Al})$. T_{Gr} is the equilibrium temperature for reaction 7, and the exponents relate to the two Al ions in both garnet and anorthite which can be replaced by Fe^{+3}. Setting the two expressions equal to each other, we have

$$(T-T_{Gr})\Delta S_{Gr} = RT \ln \frac{X^{A^2}_{Al}}{X^{G^2}_{Al}}. \quad (8)$$

Hydrothermal experiments were conducted at 740°C, 2068 bars for 42 days using a CT buffer (Table 5A). Anorthite, wollastonite, and quartz were mixed with various compositions of garnet. Refractive index measurements on the

3 K_D for anorthite-grandite is assumed to be 0.01 as previously discussed.

Table 5. Experimental results in the system grossularite-andradite with excess silica[a]

Run	T °C	Starting materials	System composition	Products
A. Cuprite-tenorite buffer, 2068 bars, 42 days				
608	740	$And_{33.3}$ + Qz + An + Wo	And_{13}	$And_{53.5}$ + Qz + An + Wo
609	740	And_{41} + Qz + An + Wo	And_{16}	$And_{53.5}$ + Qz + An + Wo
611	740	And_{100} + Qz + An + Wo	And_{29}	$And_{53.5}$ + Qz + An + Wo
B. *Air Buffer, 1 Bar, 10 days, Representative Runs*				
605B	1160	*And_{100}* + *Qz* + *An* + Wo + Hem	And_{87}	$And_{94.5}$ + Tr + Pwo + Hem + Gl
612A	1170	Run 605B	And_{87}	Pwo + Hem + Gl (Ga)[b]
612B	1170	*And_{100}* + Qz + An + Wo + Hem	And_{72}	Pwo + Gl[b]
612C	1170	*And_{100}* + Qz + *An* + Wo + Hem	And_{95}	Pwo + Hem + Gl (Ga)[b]
614A	1165	*And_{100}* + Qz + An + Wo + Hem	And_{72}	Tr + Pwo + Gl
614B	1165	*And_{100}* + Qz + *An* + Wo + Hem	And_{81}	Tr + Pwo + Hem + Gl (Ga)
614D	1165	*And_{100}* + Qz + Hem + Ca + *Cor*	And_{91}	Tr + Pwo + Hem + Gl (Ga)
615B	1155	*And_{82}* + Qz + Hem + Ca + *Cor*	And_{71}	$And_{95.5}$ + Tr + Pwo + Gl (Hem)
615C	1155	*And_{82}* + Qz + *An* + Wo + Hem	And_{80}	$And_{95.0}$ + Tr + Pwo + Gl (Hem)
616A	1145	*And_{82}* + Qz + An + Wo + Hem	And_{71}	And_{93} + Tr + Pwo + Gl (Hem)
616B	1145	*And_{82}* + Qz + Hem + Ca + *Cor*	And_{71}	Ga + Tr + Pwo + Gl (Hem)
616D	1145	*And_{82}* + Qz + Hem + Ca + *Cor*	And_{80}	$And_{94.5}$ + Tr + Pwo + Gl (Hem)
617B	1135	*And_{82}* + Qz + Hem + Ca + *Cor*	And_{71}	$And_{92.5}$ + Tr + Pwo + Gl (Hem)
617C	1135	*And_{82}* + Qz + *An* + Wo + Hem	And_{80}	And_{93} + Tr + Pwo + Gl (Hem)
618B	1125	*And_{82}* + Qz + Hem + Ca + *Cor*	And_{71}	And_{91} + Tr + Pwo + Gl (Hem)
618G	1125	And_{41} + Qz	And_{41}	Ga + Tr + Pwo + Gl
618H	1125	$And_{54.8}$ + Qz	$And_{54.8}$	$And_{93.7}$ + Tr + Pwo + Gl
619H	1115	$And_{54.8}$ + Qz	$And_{54.8}$	$And_{92.5}$ + Tr + Wo + An
619I	1115	$And_{21.3}$ + Qz	$And_{21.3}$	Ga + Tr + Wo + An
619K	1115	*And_{82}* + Qz + Hem + Ca + *Cor*	And_{61}	And_{92} + Tr + Wo + An
620B	1115	Run 616B	And_{71}	Ga + Tr + Wo + An (Hem)
620G	1115	Run 618G	And_{41}	Ga + Tr + Wo + An

[a] Mineral abbreviations as for Table 3, also: Wo wollastonite; Pwo pseudowollastonite; Tr = tridymite; Ca = Calcite; Gl = glass; *And_{100}* = 5–10% of starting materials; (Hem) = present as a minor phase in products but enclosed in garnet (hematite), enclosed in wollastonite (garnet, run 612), or much less abundant than glass (garnet, run 614), therefore considered unstable.

[b] Insufficient initial silica to produce tridymite.

garnet indicated that all garnets equilibrated to the composition $And_{53.5}$. At 2068 bars T_{Gr} is 603°C (Newton, 1966). Solution of equation 8 for ΔS_{Gr} gives 22.2 ± 2.5 cal/deg or 22.5 ± 2.5 cal/deg if anorthite solid solution is neglected. Slope calculations for reaction 7 give 20.3 ± 2 cal/deg at 1 000° K (Table 6 and Robie and Waldbaum, 1968). At 1 atm. pressure equation 8 may be solved for T giving 649°C for stability of $And_{53.5}$ with anorthite, wollastonite, and quartz (Fig. 6).

Experiments were also conducted at 1 atm. on the iron-rich end of the series. These experiments took place in a Lindberg heavy duty furnace calibrated against the melting temperature of Au. Starting minerals (Table 5B) were on the grossularite-andradite join with excess SiO_2 and consisted of either (1) mixtures of anorthite, wollastonite, reagent hematite, and quartz seeded with And_{82} or

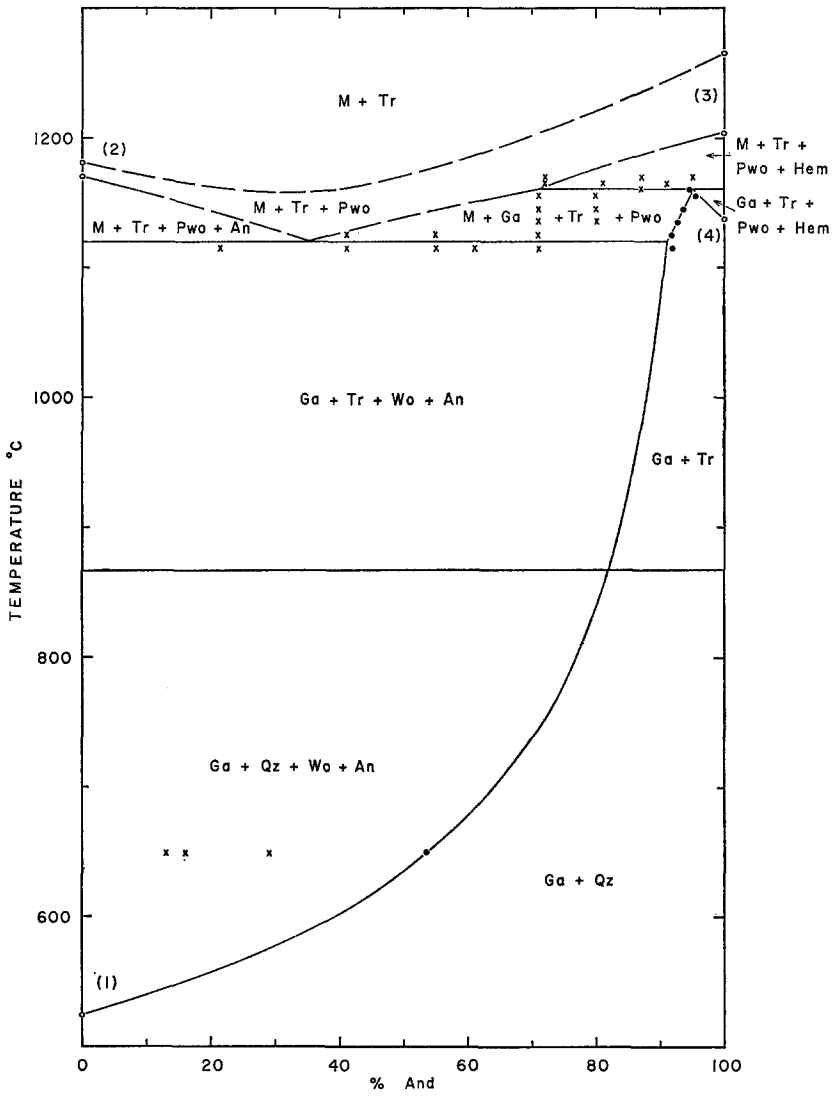

Fig. 6. Temperature-composition diagram for the pseudobinary system grossularite-andradite with excess silica under oxidizing conditions at 1 atm. Abbreviations as for Tables 3, 5, also: M melt. Dots: composition of garnet; x composition of system; open symbol: results of other studies [(1) Newton (1966), (2) Rankin and Wright (1915), (3) Phillips and Muan (1959), (4) Huckenholz and Yoder (1971)]. Solid lines: determined boundaries; dashed lines: approximate boundaries. Subsolidus lines are calculated to fit available data (see text)

And_{100} or (2) mixtures of oxides and reagent calcite seeded with And_{32}, or (3) natural grandite and quartz. Experimental charges were first sealed dry in platinum capsules and dry-pressed at 4000 bars and room temperature for one day to provide intimate contact between grains. Then the ends were cut off the capsules before they were run at temperature in an air atmosphere.

At the andradite end of the diagram the reaction:

$$Ca_3Fe_2Si_3O_{12} \rightleftarrows Fe_2O_3 + 3\ CaSiO_3 \tag{9}$$

also becomes divariant, starting at 1137° C (Huckenholz and Yoder, 1971). At 1160° C garnet melts incongruently. Compositions of garnet stable with melt were determined in the range And_{95} to And_{91}. At 1120° C no melt remains and And_{91} is stable with anorthite, wollastonite, and tridymite. The diagram of Fig. 6 shown these relations; the lines bounding the garnet stability field are experimentally determined; dashed lines are schematic.

Solution of equation 8 for ΔS_{Gr} at 1120° C gives 21.6 ± 2 cal/deg after correction for tridymite. If anorthite solid solution is excluded the result is 0.9 cal/deg higher. Such calculations cannot be made for andradite due to the limited extent of garnet solid solution over which reaction 9 applies and the unknown amount of hematite solid solution.

The divariant curve for reaction 7 in Fig. 6 has been calculated using equation 8 and an average ΔS_{Gr} of 21.9 cal/deg. The satisfactory agreement between ΔS_{Gr} calculated assuming ideal solid solution and that calculated from the slope of reaction 7 suggests that the grossularite component of grandite may be approximated by ideal ionic solid solution at temperatures not very far from those of the experiments discussed above. These results imply that calculations such as those made by Kerrick (1970) on the decomposition temperature of various members of the grossularite-andradite series based on ideal solid solution are quite reasonable.

Thermochemical Data for Garnet and Epidote

In this section an attempt will be made to calculate entropy and enthalpy of epidote group minerals and grandite garnet from an analysis of stability data. The following assumptions are made: (1) Pressure effect on ΔS_s and ΔV_s may be neglected without introducting significant errors. (2) Solid solution on the garnet octahedral sites is ideal over the range 550 to 700° C.

In these calculations thermodynamic data for all minerals besides epidote and garnet are from Robie and Waldbaum (1968). Thermal expansion is from Clark (1966). Where data are not available, thermal expansion has been estimated by analogy with comparable minerals. Thermodynamic data for water at high pressure have been taken from Burnham, Holloway, and Davis (1969).

The approach used in the calculations involved the following steps: (1) Determine the average slope of a stability curve, and apply it at a temperature at which the experimental points are closely spaced. (2) Calculate ΔS_r for the reaction using the relation $dP/dT = \Delta S/\Delta V$. (3) Using known entropies, calculate the value of entropy of the unknown mineral. (4) From the temperature and pressure at which slope was measured, determine standard free energy of reaction using the relation $d\Delta G/dP = \Delta V$. (5) From ΔG_r^0 and ΔS_r^0 calculate ΔH_r^0. (6) Using known enthalpies calculate ΔH_f^0 of the unknown material. Thermodynamic functions calculated for garnet were used in the epidote mineral calculations. Where needed, S^0 and ΔH_f^0 for garnets were extrapolated to other temperatures by drawing a curve parallel to the curve obtained by summing S^0 or ΔH_f^0 of the simplest combination of other minerals with equivalent composition.

Table 6. Molar entropy and enthalpy of garnet and epidote minerals

Mineral	Reaction, Reference[a,b]	Slope (bars/deg)	P_{eq} (bars)	T_{eq} (deg K)	S° (cal/deg)	$-\Delta H_f^\circ$[c] (K cal)
Gr	Gr + Qz = An + 2Wo [2–4]	26.5	5250	1000	181.2 ± 1.4	1590.9 ± 1.5
Gr	Sum of oxides			1000	185.7 ± 3.7	
Gr	Preferred value			1000	181.2 ± 2	1590.9 ± 1.5
And	And = Hem + 3Wo [5]	67.4	1	1410	222.9 ± 3.6	
And	Sum of oxides			1400	244.9 ± 5	
And	$S^\circ_{Gr} - S^\circ_{Cor} + S^\circ_{Hem}$			1400	241.1 ± 2	
And	Preferred value			1400	240.0 ± 5	1385.4 ± 7.0
Zo	4Zo + Qz = 5An + Gr + 2W [2, 3]	24.5	7240	1000	200.0 ± 2.1	1652.1 ± 2.2
Zo	6Zo = 6An + 2Gr + Cor + 3W [2, 6]	18.3	4800	1000	202.9 ± 1	1649.8 ± 0.9
Zo	Sum of oxides			1000	200.2 ± 4	
Zo	Preferred value			1000	201.9 ± 2	1650.6 ± 1.7
Ps_{10}	Reaction 6 [1]	30.3	3000	900	185.4 ± 3.6	1620.0 ± 3.6
Ps_9	Reaction 5 [1]	25.0	2210	900	188.3 ± 2.3	1619.9 ± 2.2
Ps_{33}	Reaction 2 [1]	20.0	1700	900	196.5 ± 3.7	1544.5 ± 4.0
Ps_0	Sum of oxides			900	187.5 ± 3.7	
Ps_{67}	Sum of oxides			900	204.3 ± 4.1	
Ps_0	Preferred value			900	183.3 ± 4	1649.6 ± 4.0
Ps_{67}	Preferred value			900	202.5 ± 6	1441.0 ± 10.0

[a] Abbreviations as in previous tables, also: Zo zoisite.

[b] References: [1] this report; [2] Boettcher (1970); [3] Newton (1966); [4] Hays (1967); [5] Huckenholz and Yoder (1971); [6] Newton (1965).

[c] Heat of formation from the elements at the temperature given.

In addition to entropy determined from phase boundaries, mineral entropies were determined using the additivity of oxides model of Fyfe, Turner, and Verhoogen (1958), including the volume correction. If the volume correction is determined at the temperature of interest, this approach provides accuracy comparable to entropy measurements based on slope determinations.

The errors recorded arise from the errors in slope measurements and equilibrium points and a 2% error assigned to entropies from additivity of oxides. In the calculations for epidote group minerals, errors in the garnet quantities are also taken into account. Errors arising from the calorimetrically determined enthalpy and entropy values are ignored because they are considerably less than errors based on the phase relations, and as long as these known values are used in other phase boundary calculations their errors tend to cancel out. Preferred values of S^0 and ΔH_f^0 are based on averaging the values determined from phase boundaries taking into account the error assigned to each (Table 6).

The entropy derived from the andradite stability curve is inconsistent with that from the sum of the oxides. A value determined from $S^\circ_{Gr} - S^\circ_{Cor} + S^\circ_{Hem}$ at 1400° supports the entropy derived from the oxide sum. Possibly the andradite stability curve involves some variable solid solution which could not be accounted for in the calculation.

Calculated Phase Relations

The Nature of Epidote Solid Solution

At this stage sufficient data are available to reach some conclusions regarding the clinozoisite-epidote solid solution and the divariant curves for their stability. In this discussion, the two energetically equal octahedral ions in the garnet formula are assumed to behave ideally.

The three octahedral positions in the epidote formula are energetically distinct. For natural epidotes Dollase (1971) and Burns and Strens (1967) have shown that Fe^{+3} is preferentially incorporated relative to Al in the M(3) site, is never more than a minor constituent in the M(1) site, and is absent in the M(2) site. Dollase (written communication) finds that the same conclusions hold for heated and synthetic epidotes. The following table gives the per cent of Fe^{+3} in M(1) for several epidotes studied, the remaining Fe^{+3} being in M(3).

Ps_{26}[4]	Natural	3.1% Dollase (writ. comm.)
Ps_{27}	Natural	6.2% Dollase (1971)
Ps_{29}	Natural	8.0% Dollase (writ. comm.)
Ps_{32}	Natural	10.3% Burns and Strens (1967)
Ps_{33}[5]	Natural	7.5% Dollase (writ. comm.)
Ps_{33}[5]	Heated 650° C, 3 kb, 28 da.	9.8% Dollase (writ. comm.)
Ps_{33}	Synthetic, 685° C, 5 kb	8.0 to 13.7% Dollase (writ. comm.)

In a general way the percentage of Fe^{+3} in M(1) increases as epidote becomes more Fe-rich. If one assumes that most of the natural epidotes crystallized at temperatures below 650° C site occupancy of Fe^{+3} in M(1) also increases somewhat with temperature. Over the range of temperatures used for this project it will be assumed that 11% of the Fe^{+3} is in M(1) in epidote of composition Ps_{33}.

The Fe-Al partitioning between garnet and epidote may be treated as an ionic single site-double site partitioning of the type discussed by Grover and Orville (1969). Two exchange reactions may be written, one between garnet and the M(3) epidote site and one between the epidote M(1) and M(3) sites. The epidote sites are identified by superscripts 1 and 3.

$$Al_{ga} + Fe^3_{ep} \rightleftarrows Fe_{ga} + Al^3_{ep}, \tag{10}$$

$$Al^1_{ep} + Fe^3_{ep} \rightleftarrows Fe^1_{ep} + Al^3_{ep}. \tag{11}$$

Equilibrium constants for these reactions are defined as follows:

$$K_{D1} = \frac{X^G_{Fe}\,\gamma\,X^{E3}_{Al}}{X^G_{Al}\,\gamma\,X^{E3}_{Fe}}, \tag{12}$$

$$K_{D2} = \frac{\gamma X^{E1}_{Fe}\,\gamma\,X^{E3}_{Al}}{\gamma X^{E1}_{Al}\,\gamma\,X^{E3}_{Fe}}. \tag{13}$$

The activity coefficients may vary as a function of composition and the site

4 Ps_{26} starting material of this report. This material heated to 650° C at 3 kb gives the same result.

5 Ps_{33} starting material of this report.

involved. If it were possible to assume that solid solution is ideal on each site, Fig. 2 could be used to put limits on the values of the K_D's.

The divariant epidote-quartz reaction has been studied at two compositions, Ps_{10} and Ps_{33}. The curve on a TX diagram may be determined using equation 8 written for the epidote-quartz reaction.

$$(T - T_{Cz})\,\Delta S_{Cz} = RT \ln \frac{X_{Al}^{G^2} X_{Al}^{A^{10}}}{\gamma X_{Al}^{E1^3} \gamma X_{Al}^{E3^4}}. \tag{14}$$

The subscript Cz denotes the iron-free reaction involving Ps_0. Approximate calculations show that if one assumes that epidote solid solution is ideal and that K_{D1} is determined from Fig. 2, K_{D2} would have to be near unity to explain the temperature differential between Ps_{10} and Ps_{33} stability at 3000 bars. Lower values of K_{D2} provide better agreement with site occupancy studies and Fig. 2. Such lower values would predict too much temperature differential between stability of Ps_{10} and Ps_{33} suggesting positive deviations from ideality ($\gamma > 1$). A comparable equation for the epidote-corundum reaction shows again that γ must be greater than one to explain the temperature differential between stability of Ps_9 and Ps_{23} (Table 3B) at 3000 bars.

If the activity coefficients could be related to a single variable, it might be possible to relate the Fe-Al partitioning data of Fig. 2 to the TX diagrams for the epidote-corundum and epidote-quartz divariant reactions. Regular (symmetrical) solution theory (Garrels and Christ, 1965, p. 44; Darken and Gurry, 1953) predicts that the activity coefficient is related to composition in the following way.

$$\ln \gamma_i = a\,(1 - X_i)^2. \tag{15}$$

If we make the further simplifying assumption that a single average value of a can be applied to each ion in each epidote site, the problem becomes more soluble.

Using a trial and error approach, one can approximately reconcile Fig. 2, epidote site population studies, and experimental equilibrium determinations, and calculate divariant curves for the epidote-quartz and epidote-corundum reactions. The following values give the partitioning curve in Fig. 2 and the divariant curves in Fig. 8: $a = 0.7$, $K_{D1} = 0.4$ $K_{D2} = 0.05$. The assumed K_D between garnet and anorthite, 0.01, has a negligible effect on the results. These results do not represent a unique solution, but only a reasonable fit of the observed data. The small discrepancies between the calculated curves and experimental data of Figs. 2 and 8 represent experimental error, imperfection in the values of a and K_D, imperfection in the model, and the ignoring of minor solid solution effects of almandine.

A similar approach at 1000 bars would require a larger value of a, 1.5 ± 0.5, suggesting that epidote solid solution is becoming more nonideal with decrease in temperature. This is consistent with the possibility of unmixing at lower temperatures. In long runs at 3000 bars and 500° C, mixtures of clinozoisite and epidote and also homogeneous epidotes of intermediate composition remained unchanged. Apparently reactions with epidotes are too sluggish below 500° C to resolve the problem with a direct experimental approach.

One cannot realistically extrapolate the slope of the epidote breakdown curve (reaction 2, Fig. 5) to increased pressure and temperature. If the K_D values

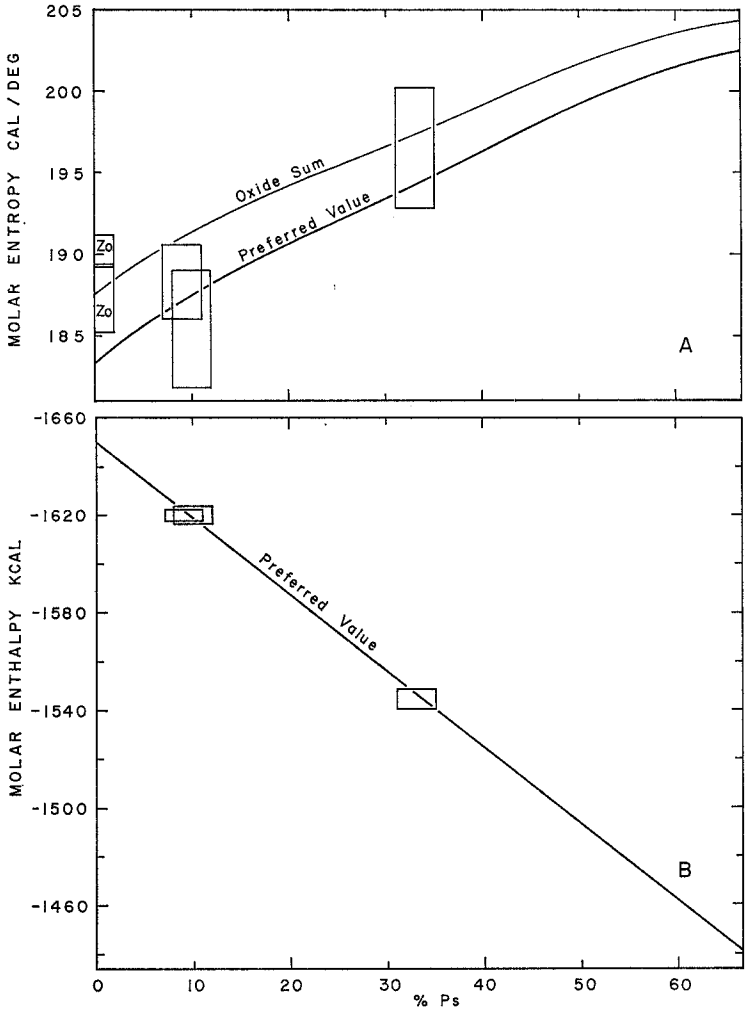

Fig. 7A and B. Thermodynamic properties at 900° K for the epidote series between Ps_0 and Ps_{67}, based on data of Table 6 and relations given in text. A entropy, B enthalpy. Values beyond Ps_{33} are hypothetical. Zoisite entropy (*Zo*) is given for comparison

remain about the same, Eq. (14) would predict a gradual steepening of the stability curve assuming a gradual decrease in a. In other words, the epidote stability curve would show greater than normal curvature in the 1000 to 5000 bar range due to the increasing degree of nonideality in epidote solid solution as temperature decreases. On the other hand, if K_{D2} increases with temperature, this would tend to counteract the steepening discussed above and produce a straighter curve. Such poorly known variations in degree of ideality and K_D values with temperature have a negative effect on the validity of the epidote entropy derived from reaction 2 (Table 6). Conversely, the entropy derived from

reactions 5 and 6 on clinozoisite are much less affected by variations in a and K_D with temperature because of the smaller amount of solid solution.

Entropy and enthalpy of zoisite and the epidote solid solution series at 900° K are given in Fig. 7. The curves shown take into account configurational entropy and enthalpy of mixing in a two-site model. K_{D2} is assumed to be 0.05 ($\Delta G_E^0 =$ 5360 cal), and ΔS_{mix} and ΔH_{miv} are given by the following relations (Grover and Orville, 1969).

$$\Delta S_{\text{mix}} = R X_{\text{Fe}}^{E1} \ln X_{\text{Fe}}^{E1} + X_{\text{Al}}^{E1} \ln X_{\text{Al}}^{E1} + X_{\text{Fe}}^{E3} \ln X_{\text{Fe}}^{E3} + X_{\text{Al}}^{E3} \ln X_{\text{Al}}^{E3}). \quad (16)$$

$$\Delta H_{\text{mix}} = \frac{(X_{\text{Fe}}^{E1} - X_{\text{Fe}}^{E3}) \Delta G_E^0}{2}. \quad (17)$$

The preferred curve for clinozoisite and epidote entropy is based mainly on the clinozoisite values and less on the epidote entropy, and drawn nearly parallel to the curve for the oxide sum.

From these curves the entropy and enthalpy of Ps_0 may be obtained (Table 6). Because zoisite and iron-free clinozoisite have essentially the same molar volume, their entropies based on the oxide sum are the same. Based on slope calculations, zoisite entropy is a little above that of the oxide sum, and Ps_0 entropy is below that of the oxide sum.

In summary, stability and partitioning data for epidote and grandite garnet may be satisfactorily explained by an ionic solution model if moderate positive deviation from ideality is assumed for epidote. There is supporting evidence, discussed above, for the ionic model for grandite solid solution. If a molecular model were used for garnet-epidote relations, it would require strong negative deviations from ideality in epidote (or positive deviations in garnet). Also the presence of two energetically different Fe-Al sites in epidote would require compositional variations in γ which could not easily be explained with a simple relationship.

A TX Diagram for Epidote

In the previous section, the divariant curves for clinozoisite-epidote decomposition were calculated for the silica-deficient and silica-excess cases (Fig. 8). The remainder of the lines on these pseudobinary diagrams under MH buffer conditions may be deduced from the experimental data. The diagrams represent those phases equal to epidote composition on the $Ca_2Al_3Si_3O_{12}(OH)$—$Ca_2Fe_3Si_3O_{12}(OH)$ join plus excess quartz or a silica-deficient mineral. Only epidote compositions may be read directly from the diagram. Assemblages marked with an asterisk are trivariant in that epidote or garnet composition may be changed independent of changes in pressure of temperature.

Any attempt to calculate approximate divariant curves for the reaction of epidote to garnet and iron oxides shows that the small value of K_{D2} leads to large temperature changes for minute shifts in epidote composition. The lines bounding the field of garnet-anorthite-magnetite-hematite-quartz and the analogous silica-deficient assemblage are drawn not quite vertical to be consistent with the andradite-rich limiting composition stable with anorthite at high temperatures (Fig. 6).

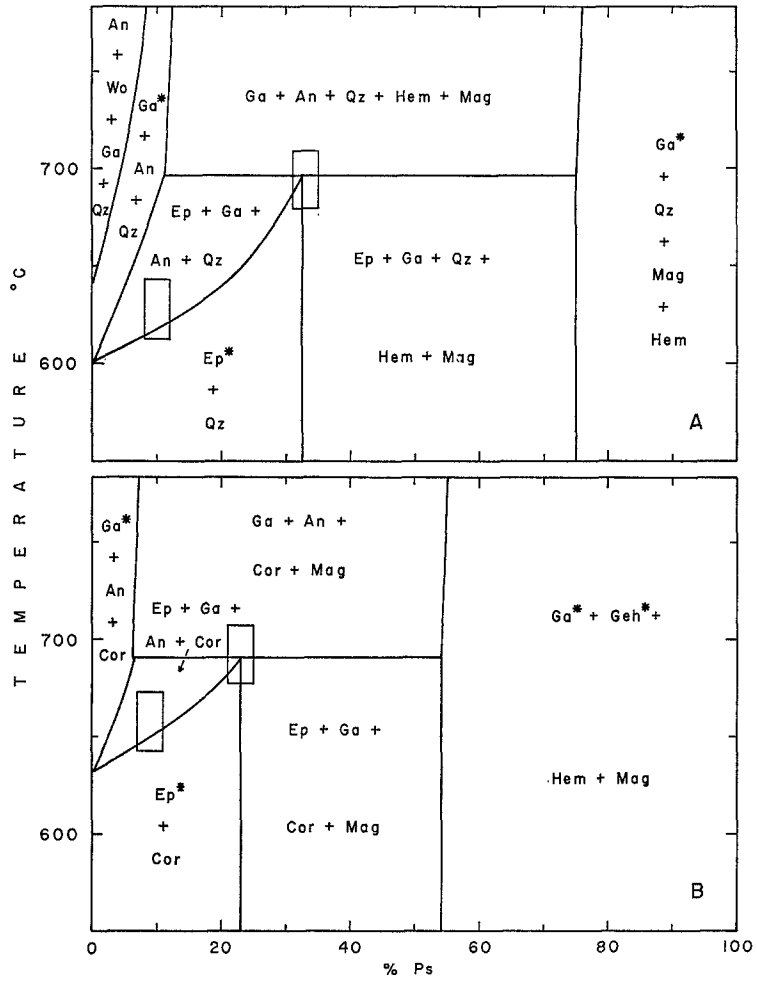

Fig. 8A and B. Temperature-composition diagrams for the pseudobinary system clinozoisite-pistacite (Ps_0–Ps_{100}) under MH buffer conditions at 3000 bars P_{H_2O}. A with excess silica, B deficient in silica. Abbreviations as for Tables 3, 5, also: Geh Fe-gehlenite. Rectangles give epidote composition and temperature for univariant and divariant reactions. Trivariant assemblages are noted with an asterisk. Only epidote composition may be read directly from the diagram

In the silica deficient assemblage epidote-garnet-magnetite-corundum the activities of Fe^{+3} and Al in epidote and garnet are fixed by the presence of the iron and aluminum oxides. Thus, in order for epidote to disappear and garnet to increase in andradite molecule, corundum must also disappear. Silica deficiency is taken up by ferric gehlenite as demonstrated by 30-day experiments at 680° C, 3000 bars which began with hematite, And_{55} or And_{82}, and portlandite, and produced ferric gehlenite, andraditic garnet, hematite, and magnetite. As discussed earlier, hematite appears to be not quite stable with magnetite and corundum under conditions of the MH buffer.

Triangular diagrams showing the phase relations of the silica-excess system Fe_2O_3—Al_2O_3—CaO were presented in an earlier study (Holdaway, 1966). It is interesting to note that even though quartz reduces the stability of epidote of a given composition, the final univariant disappearance of epidote is at about the same temperature with corundum as with quartz. This is because the limiting epidote composition is so much more aluminous in the presence of corundum.

Clinozoisite-Zoisite Equilibrium

The Fe-free analogs of reaction 5 and 6 are as follows:

$$6\ Ca_2Al_3Si_3O_{12}(OH) \rightleftarrows 2\ Ca_3Al_2Si_3O_{12} + 6\ CaAl_2Si_2O_8 + Al_2O_3 + 3\ H_2O, \quad (18)$$

$$4\ Ca_2Al_3Si_3O_{12}(OH) + SiO_2 \rightleftarrows Ca_3Al_2Si_3O_{12} + 5\ CaAl_2Si_2O_8 + 2\ H_2O. \quad (19)$$

Approximate stability curves for Fe-free clinozoisite may be calculated using the Ps_0 intercepts from Fig. 8 and slope calculations based on data of Table 6 and Robie and Waldbaum (1968). The resulting curves are shown in Fig. 9 along with their error limits. If clinozoisite solid solution were assumed to be ideal and all the iron were in the M(3) site the curves for Ps_0 would be about 5° C lower than those shown.

The stability curves for zoisite by reactions 18 and 19 (Newton, 1965, 1966) are also given in Fig. 9. The clinozoisite curves are each steeper than the analogous zoisite curve, in accord with the lower entropy calculated for clinozoisite. The curves for clinozoisite cross the zoisite curves at points A and B. The lower portions of the zoisite lines are metastable, while the upper portions of the clinozoisite lines are metastable.

The univariant reaction between clinozoisite and zoisite has proven difficult to determine experimentally. Evidence bearing on the nature of this equilibrium is summarized below.

1. Previous experimental investigations (Boettcher, 1970; Pistorius *et al.*, 1962) have shown that whether zoisite or clinozoisite forms in the Fe-free system is in large part a function of starting materials. Glasses and crystalline mixtures containing anorthite produce zoisite. When scolecite is the starting mineral, clinozoisite forms. No one has ever converted zoisite to clinozoisite or vice versa. The ease of crystallization of zoisite under conditions at which clinozoisite may be stable could result from its higher entropy, as suggested by Fyfe (1960b) for other experimental systems. The small ΔS for the reaction may inhibit conversion to the stable form.

2. The clinozoisite-zoisite equilibrium curve must be nearly vertical. According to the data of Pistorius (1961) on synthesized minerals, ΔV for the reaction is $+0.1$ cc. Extrapolation of Seki's (1959) results on natural clinozoisite and zoisite to zero iron content indicates ΔV of $+0.15$ cc. Comparable data of Myer (1966) lead to a value of $+0.3$ cc. Thus clinozoisite appears to be the high pressure phase. On the basis of the silica-excess reactions (Table 6, Fig. 8) $\Delta S°$ is 6.0 ± 5.0 cal/deg; based on the silica-deficient reactions $\Delta S°$ for the clinozoisite-zoisite reaction is

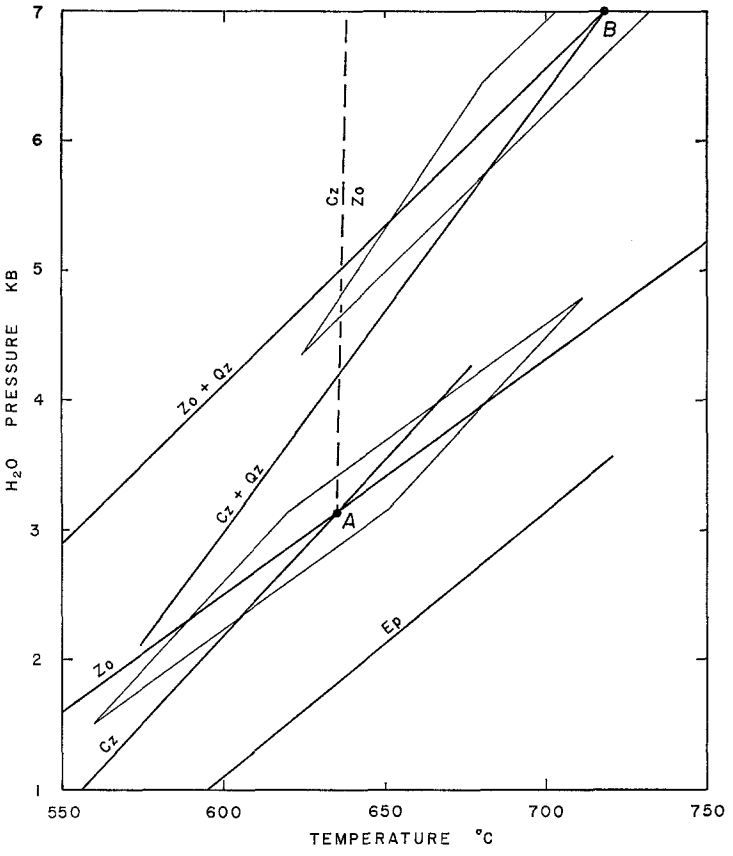

Fig. 9A and B. Stability curves for zoisite (Newton, 1965, 1966) and epidote and calculated stability curves for clinozoisite (Ps_0). Error ranges for the intersections A and B are shown by fine lines. The dashed line represents the approximate position of the clinozoisite-zoisite reaction

5.7 ± 2.1 cal/deg[6]. Using a $\Delta S°$ of 6 cal/deg and a ΔV of 0.2 cc., the calculated slope of the reaction is about $+1300$ bars/deg.

3. The points of intersection between the clinozoisite and zoisite stability curves (A, Fig. 9) and between the clinozoisite-quartz and zoisite-quartz curves (B, Fig. 9) should lie on the clinozoisite-zoisite curve. However, due to the small angles of intersection between the curves which determine A and B, there are large possible errors. The reliability of point A is much better than that of point B, because the silica-excess reactions are less accurately known that the silica-deficient reactions.

The dashed curve of Fig. 9 best accounts for all the evidence presented there. It has a slope of 1300 bars/deg. and passes through point A and within the error

6 Error contributed by grossularite entropy has been subtracted from the error, because grossularite is eliminated between the clinozoisite and zoisite reactions. Silica-excess and silica-deficient reactions for zoisite and clinozoisite are considered separately because of the consistent 2 to 3 cal/deg difference between entropy calculated from the two types of reaction, which may have resulted from an error in entropy of one of the participant minerals.

field of point B. The estimated error in this approximate boundary between clinozoisite and zoisite stability is $\pm 75°$ C. The significance of the conclusion that zoisite does not become stable until some temperature above 560° C will be discussed below.

Application to Metamorphic Petrology

For the purposes of this study, the following compositional subdivision of the Al-Fe epidote minerals will be made.

Al-Zoisite	Ps_0 to $Ps_{2.5}$
Fe-Zoisite	$Ps_{2.5}$ to Ps_5
Al-Clinozoisite	Ps_0 to Ps_5
Fe-Clinozoisite	Ps_5 to Ps_{10}
Al-Epidote	Ps_{10} to $Ps_{22.5}$
Fe-Epidote	$Ps_{22.5}$ to Ps_{35}

Fe-zoisite is the same as ferrian zoisite (Myer, 1966). The remaining compositional boundaries are arbitrary. Myer (1966) and Seki (1959) provide optical and X-ray methods for distinguishing between orthorhombic and monoclinic epidote minerals.

With more recent studies and more precise methods of identification and analysis, the composition (and perhaps the occurrence) of zoisite is becoming more restricted, and that of clinozoisite is becoming less restricted. Some Al-clinozoisites may have been misidentified as zoisite on the basis of low 2 V. In order to dstinguish between zoisite and clinozoisite, one must either be able to measure an extinction angle or have a good quality X-ray pattern. Great care is required to distinguish zoisite from clinozoisite in fine-grained low-grade metamorphic rocks or in altered feldspars.

Occurrence of Epidote Minerals in Metamorphic Rocks

An attempt is made below to relate occurrence of epidote minerals to metamorphic facies using Turner (1968) as the principal reference. Clinozoisite and epidote first appear at low to moderate pressures with the decomposition of zeolites at the beginning of the prehnite-pumpellyite metagraywacke facies. At higher pressures clinozoisite and epidote first become important minerals in conditions transitional between the glaucophane schist and greenschist facies as lawsonite begins to disappear (Ernst, Seki, Onuki, and Gilbert, 1970).

Epidote has often been reported to be of Fe-rich composition at lowest grades changing to variable compositions at higher grades (Miyashiro and Seki, 1958), or to more aluminous compositions at higher grades (Holdaway, 1965; Ernst *et al.*, 1970). There are several factors which could affect epidote composition in zoisite-free rocks. (1) Early Fe-rich cores in epidote of low grade rocks noted by Ernst *et al.* and by Brown (1967) probably result from the fact that zeolites and lawsonite reacting to form the first epidote are not Fe-bearing. The Ca-Al silicates react with Fe-bearing minerals such as glaucophane and actinolite to form Fe-epidote and the Ca-Al silicates persist stably with the Fe-epidote for a short temperature interval before beginning to break down to more aluminous epidote and clinozoisite. (2) Within conditions of clinozoisite-epidote stability, bulk

composition and f_{O_2} control the composition of the epidote mineral. (3) Immiscibility may inhibit the formation of Al-epidote in low-grade conditions under which clinozoisite and Fe-epidote are stable. (4) At least in simple epidote decomposition reactions, clinozoisite breaks down at lower temperatures than epidote. Points 2 and 3 will be discussed in more detail in the last part of this report.

Clinozoisite and epidote react with albite at the beginning of the almandine-amphibolite facies of regional metamorphism or the hornblende hornfels facies of contact metamorphism. The persistence of epidote is in large part a function of the Ca/Na ratio of the rock. In calcic rocks the divariant reaction with plagioclase will allow persistence of epidote to higher grades. If grossularitic garnet is not produced in the breakdown reaction, then some other phase must react with epidote and plagioclase. Several such reactions have been discussed by Kretz (1963) and Kerrick (1970). Only in calcareous rocks will the reactions presented in this paper occur, and in these rocks epidote and clinozoisite persist to the highest metamorphic grades, within the sillimanite zone of associated pelitic rocks. Under such conditions the main factors which lower stability of epidote are albite molecule in plagioclase, P_{H_2O} less than P_{tot}, and reducing conditions. Comparison of Figs. 3 and 8 shows that epidote of a given composition breaks down at somewhat lower temperatures under reducing conditions than under oxidizing conditions.

Clinozoisite and epidote are also observed as stable minerals in some group C eclogites associated with glaucophane schists and greenschists (Coleman, Lee, Beatty, and Brannock, 1965; Green, Lockwood, and Kiss, 1968).

Because of its less common occurrence, generalization on the natural conditions of zoisite formation is more difficult. Zoisite apparently does not occur in glaucophane schist, greenschist, prehnite-pumpellyite, or low pressure contact metamorphism. The best-documented occurrences of zoisite are in impure calcareous rocks and calcareous pelitic schists in the middle grades of high pressure Barrovian metamorphism (Harpum, 1954; Kennedy, 1949; Misch, 1964; Harker, 1932). Harpum indicates that in Tanganyika zoisite begins to appear at higher grades than epidote and persists to higher grades than epidote. Zoisite is present with quartz in the almandine amphibolite facies and at some localities in the albite-epidote amphibolite facies (greenschist-amphibolite transition of Turner, 1968). In the latter facies zoisite occurs with albite and, in rocks of appropriate composition, with almandine or hornblende. In at least one case (Kennedy, 1949) the designation of grade is based solely on the occurrence of zoisite-albite. Reducing conditions are an important factor in some zoisite occurrences as indicated by presence of graphite in zoisite-bearing calc-schists.

Zoisite is also a mineral of probable primary origin in some group B eclogites associated with rocks of the almandine amphibolite facies. Zoisite breaks down in metamorphic rocks according to reactions comparable to those discussed for epidote and clinozoisite.

Clinozoisite-Zoisite Relations

The results of this experimental study suggest that zoisite is a high-temperature, high-pressure mineral stable above $635 \pm 75°C$ and 3 ± 1 kb. This conclusion is

consistent with the more common occurrence of clinozoisite than zoisite in low-grade rocks. However, it is not necessarily consistent with occurrence of zoisite in high pressure rocks of the albite-epidote amphibolite facies. Such rocks probably crystallized at $P_{H_2O} = P_{tot}$ between 5 and 8 kb. The best experimental evidence for the beginning of the almandine amphibolite facies is based on staurolite-forming reactions. At 7 kb staurolite first appears with quartz from reaction of chloritoid and aluminum silicate at 550° C according to Richardson (1968). Hoschek (1969) showed that Fe-rich chlorite[7] and muscovite react to staurolite, biotite, and quartz at 565° C at 7 kb. Nothing is yet known of the effect of Mg-Fe solid solution on staurolite stability at moderately high pressures. Conflicting evidence is provided by Hsu (1968) whose data indicate that almandine, a mineral stable well before the beginning of the almandine amphibolite facies, does not become stable before a temperature of 600° C at moderate pressures. Again the effect of Mg is not known. The preponderance of experimental results suggests strongly that high pressure albite-epidote amphibolite facies rocks, and therefore some zoisite, crystallized at temperatures below 565° C.

Morgan (1970) describes an occurrence of high pressure metamorphism in which chloritoid without aluminum silicate is developed in the same area as zoisite. Zoisite, in some occurrences; *e.g.*, zoisite with serpentine (Temple, 1966) and zoisite with prehnite (Watson, 1942) may have persisted metastably from higher temperatures than those implied by coexisting minerals.

There are several possible reasons for the apparent inconsistency between clinozoisite-zoisite stability deduced from equilibria of epidote minerals and that deduced from the natural occurrence of zoisite: (1) An unfortunate combination of experimental errors could lower zoisite stability considerably. (2) Zoisite may have crystallized metastably in the field of clinozoisite but not far below the phase boundary. (3) If the reaction of zoisite, albite and quartz to form oligoclase is being used to define the beginning of the almandine-amphibolite facies at higher pressure, then the relatively flat zoisite stability curve will stabilize albite-epidote amphibolites to higher temperatures. (4) Nonhydrostatic stress could favor zoisite relative to clinozoisite (Coe and Paterson, 1968). Clearly the present results on zoisite-clinozoisite are tentative and must await additional study of field and experimental relations.

The effect of adding small amounts of ferric iron to the zoisite-clinozoisite reaction produces a divariant equilibrium. Ps_{10} curves intersect zoisite curves at still higher temperatures than the intersections in the Fe-free system, indicating that progressively higher temperatures are required to produce Fe-zoisite (Ehlers, 1953, Fig. 2). This provides an explanation for the Fe-zoisite, Al-epidote occurrence in Norway so well documented by Myer (1966). Myer believes this assemblage (zoisite about $Ps_{3.5}$ with epidote Ps_{12} and quartz) represents equilibrium. Occurrence of Fe-zoisite and Al-epidote has been noted elsewhere (*e.g.*, Harpum, 1954). As stability curves for more Fe-rich clinozoisite crosse the zoisite curve, Fe-epidote becomes stable with a progressively more Fe-rich orthorhombic phase. For the Norwegian rocks discussed by Myer the stability curve for Fe-zoisite ($Ps_{3.5}$) plus quartz must lie at slightly lower temperatures than that for pure

7 If the results of Hsu (1968) are too high by as much as 50° C, this chlorite could be metastable.

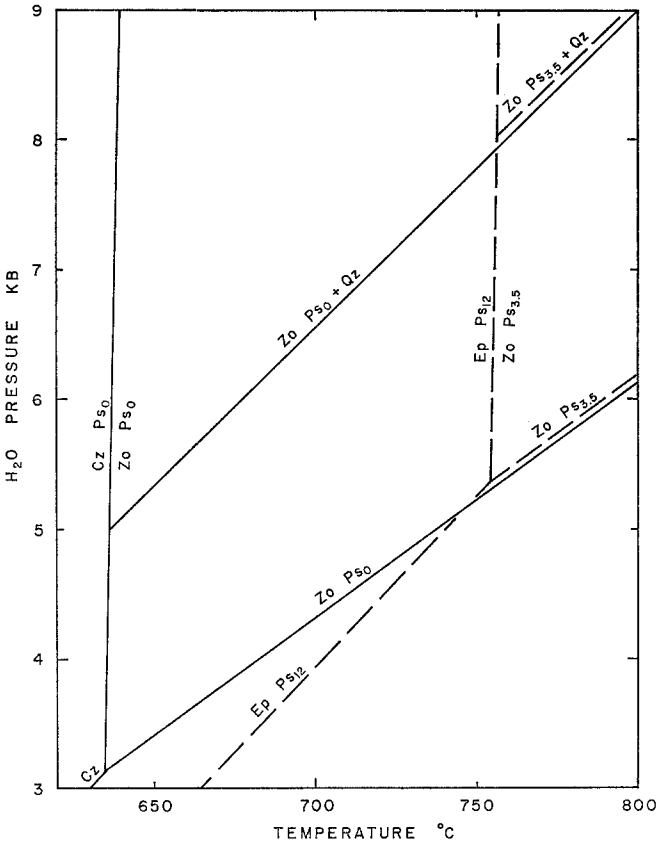

Fig. 10. Schematic relations between orthorhombic and monoclinic epidote minerals. Solid lines relate to stability of zoisite with composition Ps_0, dashed lines zoisite $Ps_{3.5}$. Steep lines are representative lines in the divariant clinozoisite fractional decomposition to zoisite

zoisite plus quartz. The relations are shown schematically in Fig. 10 where it can be seen that the Norwegian assemblage crystallized on a steep line beginning at $750 \pm 75°C$ and 8 ± 1 kb. The increase in pressure and temperature necessary to enlarge the zoisite composition field and allow zoisite to coexist with Ps_{12} is consistent with the rarity of more Fe-rich zoisites and zoisite with more Fe-rich epidote. Conversely, more precise data on the stability of zoisite-epidote assemblages will provide a useful geothermometer and minimum geobarometer.

It is also interesting to note that the only zoisite more Fe-rich than the Norwegian zoisites that is reported by Myer is of Ps_5 composition from a quartz vein cutting an eclogite. Nitsch and Winkler (1965) suggested on the basis of their results, that all monoclinic epidote would ultimately become less stable than zoisite. However, Fig. 9 shows that this is not likely for conditions typical of zoisite-bearing (group B) eclogites. A more likely explanation for the absence of epidote in such eclogites is low f_{O_2}. In any event, the maximum content of Fe^{+3}

in zoisite of eclogites should allow determination of a minimum pressure and temperature of formation.

Effect of f_{O_2} and Bulk Composition on Epidote

As mentioned previously, f_{O_2} and bulk composition have a controlling influence on the composition of epidote, especially when all compositions in the monoclinic series are stable. Bulk composition of the rock determines the epidote composition, and f_{O_2} determines the maximum possible Fe content of the epidote (Figs. 3, 8). Only if the epidote coexists with an Fe-excess mineral such as magnetite or hematite can we conclude that its composition is a function of f_{O_2} alone. The situation is further complicated by the fact that bulk composition may in large part control f_{O_2}. If epidote is initially the only Fe-bearing mineral in the rock, the decomposition of the epidote under conditions of a system closed with respect to O_2 and H_2 will ultimately produce a hematite-bearing assemblage buffered by magnetite-hematite.

Epidote Immiscibility

The partial convergence of the epidote and clinozoisite-quartz stability curves with decreasing pressure and temperature (Fig. 5) implies that epidote solid solution is becoming more nonideal as temperature decreases. As discussed previously, this is consistent with immiscibility between clinozoisite and epidote at lower temperatures. However, there are no experimental data that prove an immiscibility within the range of temperatures in which epidote occurs in nature.

Several field studies concerning epidote immiscibility are in conflict. Under conditions of the chlorite zone Strens (1963, 1964) found a gap between Ps_{13} and Ps_{24}; Holdaway (1965) found a gap between Ps_{10} and Ps_{29}; Brown (1967) found no gap, but his data show no compositions between Ps_{21} and Ps_{26}; and Keith, Muffler, and Cremer (1968) analyzed compositions of Ps_{20} and Ps_{32}. A possible interpretation of these data is an assymetrical solvus with its top at Ps_{22}. At conditions of higher grade than the chlorite zone there appears to be no evidence for a solvus.

Acknowledgments. This study was supported by the National Science Foundation (Grant GP-1371) and by Southern Methodist University. Some of the equipment was purchased under NASA Grant NCR-44-007-006. I wish to thank E. H. Erikson and H. Haas for their assistance in the laboratory, and D. C. Thorstenson and H. Haas for their contributions to discussions concerning the work. I thank W. A. Dollase for making results of his epidote site population studies available before publication. I am grateful to B. W. Evans and D. M. Kerrick for many helpful suggestions in their critical reviews of the manuscript.

References

Boettcher, A. L.: The system CaO-Al_2O_3-SiO_2-H_2O at high pressures and temperatures J. Petrol. **11**, 337–379 (1970).

Brown, E. H.: The greenschist facies in part of eastern Otago, New Zealand. Contr. Mineral. and Petrol. **14**, 259–292 (1967).

Burnham, C. W.: Lattice constant refinement. Carnegie Inst. Wash. Year Book **61**, 132–135 (1962).

Burnham, C. W., Holloway, J. R., Davis, N. F.: Thermodynamic properties of water to 1000°C and 10,000 bars. Geol. Soc. Am. Spec. Paper **132**, 96 p. (1969).

Burns, R. G., Strens, R. G. J.: Structural interpretation of polarized absorption spectra of the Al-Fe-Mn-Cr epidotes. Mineral. Mag. **36**, 204–226 (1967).

Clark, S. P., ed.: Handbook of physical constants. Geol. Soc. Am. Mem. **97**, 587 p. (1966).

Coe, R. S., and Paterson, M. S.: Coherent polymorphic transitions under nonhydrostatic stress: the α-β inversion in quartz. Am. Geophys. Union Trans. **49**, 761 (1968).

Coleman, R. G., Lee, D. E., Beatty, L. B., Brannock, W. W.: Eclogites and eclogites: their differences and similarities. Geol. Soc. Am. Bull. **76**, 483–508 (1965).

Darken, L. S., Gurry, R. W.: Physical chemistry of metals, 535 p. New York: McGraw-Hill 1953.

Deer, W. A., Howie, R. A., Zussman, J.: Rock-forming minerals, vol. 1, Ortho- and ring silicates, 333 p. New York: John Wiley 1962.

Dollase, W. A.: Refinement of the crystal structures of epidote, allanite, and hancockite. Am. Mineralogist **56**, 447–464 (1971).

Ehlers, E. G.: An investigation of the stability relations of the Al-Fe members of the epidote group. J. Geol. **61**, 231–251 (1953).

Ernst, W. G., Seki, Y., Onuki, H., Gilbert, M. C.: Comparative study of low-grade metamorphism in the California coast ranges and the outer metamorphic belt of Japan. Geol. Soc. Am. Spec. Papers **124**, 276 p. (1970).

Eugster, H. P., Wones, D. R.: Stability relations of the ferruginous biotite, annite. J. Petrol. **3**, 82–125 (1962).

Fyfe, W. S.: Stability of epidote minerals. Nature **87**, 497 (1960a).

Fyfe, W. S.: Hydrothermal synthesis and determination of equilibrium between minerals in the subsolidus region. J. Geol. **68**, 553–566 (1960b).

Fyfe, W. S., Turner, F. J., Verhoogen, J.: Metamorphic reactions and metamorphic facies. Geol. Soc. Am. Mem. **73**, 259 p. (1958).

Garrels, R. M., Christ, C. L.: Solutions, minerals, and equilibria, 450 p. New York: Harper & Row 1965.

Green, D. H., Lockwood, J. P., Kiss, E.: Eclogite and almandine-jadeite-quartz rock from the Guajira peninsula, Columbia, South America. Am. Mineralogist **53**, 1320–1335 (1968).

Grover, J. E., Orville, P. M.: The partitioning of cations between coexisting single and multisite phases with application to the assemblages: orthopyroxene-clinopyroxene and orthopyroxene-olivine. Geochim. Cosmochim. Acta **33**, 205–226 (1969).

Harker, A.: Metamorphism, 362 p. London: Methuen 1932.

Harpum, J. R.: Formation of epidote in Tanganyika. Geol. Soc. Am. Bull. **65**, 1075–1092 (1954).

Hays, J. F., Lime-alumina-silica. Carnegie Inst. Wash. Year Book **65**, 234–239 (1967).

Holdaway, M. J.: Basic regional metamorphic rocks in part of the Klamath Mountains, northern California. Am. Mineralogist **50**, 953–977 (1965).

Holdaway, M. J.: Hydrothermal stability of clinozoisite plus quartz. Am. J. Sci. **264**, 643–667 (1966).

Holdaway, M. J.: Stability of andalusite and the aluminum silicate phase diagram. Am. J. Sci. **271**, 97–131 (1971).

Hoschek, G.: The stability of staurolite and chloritoid and their significance in metamorphism of pelitic rocks. Contr. Mineral. and Petrol. **22**, 208–232 (1969).

Hsu, L. C.: Selected phase relationships in the system Al-Mn-Fe-Si-O-H: a model for garnet equilibria. J. Petrol. **9**, 40–83 (1968).

Huckenholz, H. G., Yoder, H. S.: Andradite stability relations in the $CaSiO_3$-Fe_2O_3 join up to 30 kb. Neues Jahrb. Mineral. Abhandl. **114**, 246–280 (1971).

Huebner, J. S.: Buffering techniques for hydrostatic systems at elevated pressures. *In* Ulmer, G. C., ed.: Research techniques for high pressure and high temperature, 367 p. Berlin-Heidelberg-New York: Springer 1971.

Keith, T. E. C., Muffler, L. J. P., Cremer, M.: Hydrothermal epidote formed in the Salton Sea geothermal system, California. Am. Mineralogist **53**, 1635–1644 (1968).

Kennedy, W. Q.: Zones of progressive regional metamorphism in the Moine schists of the western Highlands of Scotland. Geol. Mag. **86**, 43–56 (1949).

Kerrick, D. M.: Contact metamorphism in some areas of the Sierra Nevada, California. Geol. Soc. Am. Bull. **81**, 2913–2938 (1970).

Kretz, R.: Note on some equilibria in which plagioclase and epidote participate. Am. J. Sci. **261**, 973–982 (1963).

Liou, J. G.: Synthesis and stability relations of epidote, $Ca_2Fe^{+3}Al_2Si_3O_{13}H$. Am. Geophys. Union Trans. **53**, 538–539 (1972).

Merrin, S.: Experimental investigation of epidote paragenesis. Diss. Penn. State Univ. 1962.

Myer, G. H.: X-ray determinative curve for epidote. Am. J. Sci. **263**, 78–86 (1965).

Myer, G. H.: New data on zoisite and epidote. Am. J. Sci. **264**, 364–385 (1966).

Misch, P.: Stable association wollastonite-anorthite and other calc-silicate assemblages in amphibolite facies crystalline schists of Nanga Parbat, northwest Himalayas. Contr. Mineral. and Petrol. **10**, 315–356 (1964).

Miyashiro, A., Seki, Y.: Enlargement of the composition field of epidote and piemontite with rising temperature. Am. J. Sci. **256**, 423–430 (1958).

Morgan, B. A.: Petrology and mineralogy of eclogite and garnet amphibolite from Puerto Cabello, Venezuela. J. Petrol. **11**, 101–145 (1970).

Newton, R. C.: The thermal stability of zoisite. J. Geol. **73**, 431–441 (1965).

Newton, R. C.: Some calc-silicate equilibrium relations. Am. J. Sci. **264**, 204–222 (1966).

Nitsch, K. H., Winkler, H. G. F.: Bildungsbedingungen von Epidot und Orthozoisit. Contr. Mineral. and Petrol. **11**, 470–486 (1965).

Phillips, B., Muan, A.: Phase equilibria in the system CaO-iron oxide-SiO_2 in air. J. Am. Ceram. Soc. **42**, 413–423 (1959).

Pistorius, C. W. F. T.: Synthesis and lattice constants of pure zoisite and clinozoisite. J. Geol. **69**, 604–609 (1961).

Pistorius, C. W. F. T., Kennedy, G. C.: Stability relations of grossularite and hydrogrossularite at high temperatures and pressures. Am. J. Sci. **258**, 247–257 (1960).

Pistorius, C. W. F. T., Kennedy, G. C., Sourirajan, S.: Some relations between the phases anorthite, zoisite, and lawsonite at high temperatures and pressures. Am. J. Sci. **260**, 44–56 (1962).

Rankin, G. A., Wright, F. E.: The ternary system CaO-Al_2O_3-SiO_2. Am. J. Sci. **189**, 1–79 (1915).

Richardson, S. W.: Staurolite stability in a part of the system Fe-Al-Si-O-H. J. Petrol. **9**, 467–488 (1968).

Robie, R. A., Waldbaum, D. R.: Thermodynamic properties of minerals and related substances at 298.15° K (25.0° C) and one atmosphere (1.013 bars) pressure and at higher temperatures. U. S. Geol. Surv. Bull. **1259**, 256 p. (1968).

Seki, Y.: Relation between chemical composition and lattice constants of epidote. Am. Mineralogist **44**, 720–730 (1959).

Skinner, B. J.: Physical properties of end-members of the garnet group. Am. Mineralogist **41**, 428–436 (1956).

Strens, R. G. J.: Some relations between members of the epidote group. Nature **198**, 80–81 (1963).

Strens, R. G. J.: Epidotes of the Borrowdale volcanic rocks of central Borrowdale. Mineral. Mag. **33**, 868–886 (1964).

Strens, R. G. J.: Stability relations of the Al-Fe epidotes. Mineral. Mag. **35**, 464–475 (1965).

Temple, A. K.: Zoisite-rutile rock from Los Angeles County, California. Am. Mineralogist **51**, 1028–1034 (1966).

Turner, F. J.: Metamorphic petrology, 403 p. New York: McGraw-Hill 1968.

Turnock, A. C., Eugster, H. P.: Fe-Al oxides: phase relationships below 1000° C. J. Petrol. **3**, 533–565 (1962).

Watson, K. DeP.: Zoisite-prehnite alteration of gabbro. Am. Mineralogist **27**, 638–645 (1942).
Winkler, H. G. F., Nitsch, K. H.: Zoisitbildung bei der experimentellen Metamorphose. Naturwissenschaften **49**, 605 (1962).
Winkler, H. G. F., Nitsch, K. H.: Bildung von Epidote. Naturwissenschaften **50**, 612–613 (1963).

Note Added in Proof. Another possible explanation for the inconsistency between clinozoisite-zoisite stability deduced from experimental results and that determined from field occurrence relates to the assumed slope of the equilibrium curve. At high pressure and temperature ΔV for the reaction could conceivably become negative allowing a steep negative slope for the phase boundary. This would help to explain the occurrences of zoisite in high pressure rocks of the albite-epidote amphibolite facies.

Prof. Dr. M. J. Holdaway
Department of Geological Sciences
Southern Methodist University
Dallas, Texas 75222
U.S.A.